1971

Low frequency lumped element directional couplers

Constantine Rodolph Jenkins

Department:

LOW FREQUENCY LUMPED ELEMENT DIRECTIONAL COUPLERS

BY

CONSTANTINE RODOLPH JENKINS, 1933-

A THESIS

Presented to the Faculty of the Graduate School of the

UNIVERSITY OF MISSOURI-ROLLA

In Partial Fulfillment of the Requirements for the Degree

MASTER OF SCIENCE IN ELECTRICAL ENGINEERING

1971

Approved by

James E. Adair (Advisor) Thomas P. Van Doren

R. M. Rakestraw

ABSTRACT

Lumped element directional couplers are desirable at frequencies below the VHF range because they eliminate the large physical size necessary for the distributed element directional couplers. The purpose of this work is to describe the theory and design of such low frequency lumped element directional couplers.

A model for the coupler is developed and the equations which describe it are derived. Scattering matrices for one and two section couplers are obtained. Computer solutions for three section couplers are presented. Experimental results for one, two, and three section couplers are presented and comparison with theory are made. Comparisons of theoretical and experimental work show that lumped element couplers are useful at low frequencies.

ACKNOWLEDGMENTS

The author wishes to express his appreciation to the members of his committee, especially the chairman, Dr. James E. Adair, for his guidance and direction throughout this project. A special note of thanks is given to Mr. Walt Henry for his contribution in making the circuit boards used in this prototype.

TABLE OF CONTENTS

Page

ABSTRACT ii

ACKNOWLEDGEMENTS iii

LIST OF ILLUSTRATIONS. vi

I. INTRODUCTION 1

II. REVIEW OF LITERATURE 3

III. DISCUSSION 4

A. Directional Coupler Theory 4

B. The Model. 6

C. Single Section Directional Coupler 7

1. General Equations. 11
2. Conditions for Directional Coupling. . . 15
3. Determination of the Characteristic Impedance. 15
4. Scattering Matrix. 17
5. Determination of the Cutoff Frequency. . 19
6. Coupling, Loss, and Directivity. 19
7. Coupling and Bandwidth 21
8. Coupler Design 21
9. Matching Network 24

D. Two Section Directional Coupler. 28

1. Conditions for Cascading Sections. . . . 28
2. General Equations. 30
3. Scattering Matrix. 33
4. Coupling and Insertion Loss. 34
5. Two Sections With Identical k's. 35
6. Two Sections With Different k's. 36

E. Three Section Directional Coupler. 39

F. Experimental Procedure 43

G. Experimental Results 44

page

IV. SUMMARY AND CONCLUSIONS. 53

V. SUGGESTIONS FOR FURTHER STUDY. 55

BIBLIOGRAPHY 56

VITA 58

LIST OF ILLUSTRATIONS

Figure		Page
1	Block Diagram of a Four Port Directional Coupler.	5
2	Schematic Representation of a Section of Two Coupled Transmission Lines	8
3	Model for Directional Coupler.	9
4	Equivalent Circuit of a Single Section Directional Coupler.	10
5	Coupling and Insertion Loss Versus Normalized Frequency for a Single Section Coupler With k Varied as a Parameter	22
6	Normalized Z_o Versus Normalized Frequency.	25
7	Matching Network With Low Pass Prototype.	27
8	Schematic Representation of a Two Section Directional Coupler.	29
9	Coupling Versus Normalized Frequency for a Two Section Coupler with $k_1=k_2=0.316$.	37
10	Coupling Versus Normalized Frequency for a Two Section Coupler with $k_1=0.316$ and k_2 Varied as a Parameter	38
11	Coupling Versus Normalized Frequency for a Three Section Coupler With $k_1=k_2=k_3=0.316$	41
12	Coupling Versus Normalized Frequency for a Three Section Coupler With $k_2=0.316$ and $k_1=k_3$ varied as a parameter . . .	42
13	Schematic Representation of a Single Section Coupler and its Matching Network.	45

Page

14 Block Diagram of Measurement Arrangement. 46

15 Measured Coupling, Directivity, and Insertion Loss Versus Frequency for a Single Section Coupler 47

16 Measured Coupling, Directivity and Insertion Loss Versus Frequency For a Two Section Coupler. 49

17 Measured Coupling, Directivity, and Insertion Loss Versus Frequency for a Three Section Coupler. 51

18 Prototype of the Three Section Directional Coupler With its Matching Network. 52

I. INTRODUCTION

The theory and applications of directional couplers at microwave frequencies has been studied for many years[1-5]. Applications have been limited to frequencies in and above the VHF range because large physical sizes of the distributed elements are necessary for their construction at frequencies below the VHF range. This size limitation can be eliminated by the use of lumped elements in place of the distributed elements. The purpose of this work is to describe the theory and design of such low frequency lumped element directional couplers.

The model for the coupler is a pair of coupled transmission lines where the distributed self and mutual inductances have been replaced by a transformer and the distributed capacitances have been replaced by lumped capacitors.

The coupled mode equations which describe the behavior of the coupler are derived. The boundary conditions necessary for directional coupling are then applied and a solution in terms of a scattering matrix is obtained. The case of cascaded sections is next considered. Scattering matrices for two section couplers having different coupling coefficients are presented. Plots of the coupling for three section couplers are also shown.

To show the validity of the model, experimental data for one, two, and three sectional directional couplers having equal coupling coefficients are presented and comparisons are made with calculated values. These results show that at low frequencies the lumped element model can be used as a directional coupler.

II. REVIEW OF LITERATURE

Early studies of wave propogation over a system of transmission lines led to the development of directional couplers[1-5]. Studies of directional couplers were concerned primarily with obtaining their characteristics and providing the design parameters necessary for their construction[6-7]. Directional couplers were first used to sample energy along transmission lines in order to determine the characteristics of the line under operating conditions.

With increasing technology, directional couplers were developed using structures such as coupled coaxial lines and strip lines[8-11]. Waveguide couplers were developed for use with that type of transmission system[12]. The hybrid coupler, which uses both lumped and distributed elements, are used at microwave frequencies[4,13,14].

Lumped element couplers are being used at microwave frequencies[15-16]. At frequencies in the gigahertz range, the lumped elements are physically small enough to be built into an integrated circuit package which may contain other circuitry. Some analysis has been performed on lumped element directional couplers[17]. The analysis uses a matrix approach and provides a good general theoretical discussion of lumped element couplers. Design procedures and experimental results are still lacking for low frequency lumped element directional couplers.

III. DISCUSSION

A. Directional Coupler Theory

A directional coupler is a four port device in which one of its output ports will respond to an input wave traveling in a given direction but will not respond to a wave traveling in the opposite direction[1]. A block diagram of a four port directional coupler is shown in Figure 1. From this figure it can be seen that the four port coupler is a symmetrical, bilateral device. That is, any one of the ports may be considered the input port and the other three as the output ports. For the purpose of this discussion, port one will be considered the input port.

Four port couplers can be designed in one of two ways. First, the codirectional coupler is one in which the forward wave in the main line is coupled to a forward wave in the coupled line. For example, an input wave at port one (a_1^+) would be coupled to port four (a_4^+) but not to port three (a_3^-). Second, the contradirectional coupler is one in which the forward wave in the main line is coupled as a backward traveling wave in the coupled line. For example, an input wave at port one (a_1^+) would be coupled to port three (a_3^-) but not to port four (a_4^+). In both cases port two (a_2^+) would be the main feed wave. Throughout this work only the contradirectional coupler will be discussed. Therefore, the definitions which follow are in terms of this type of coupler.

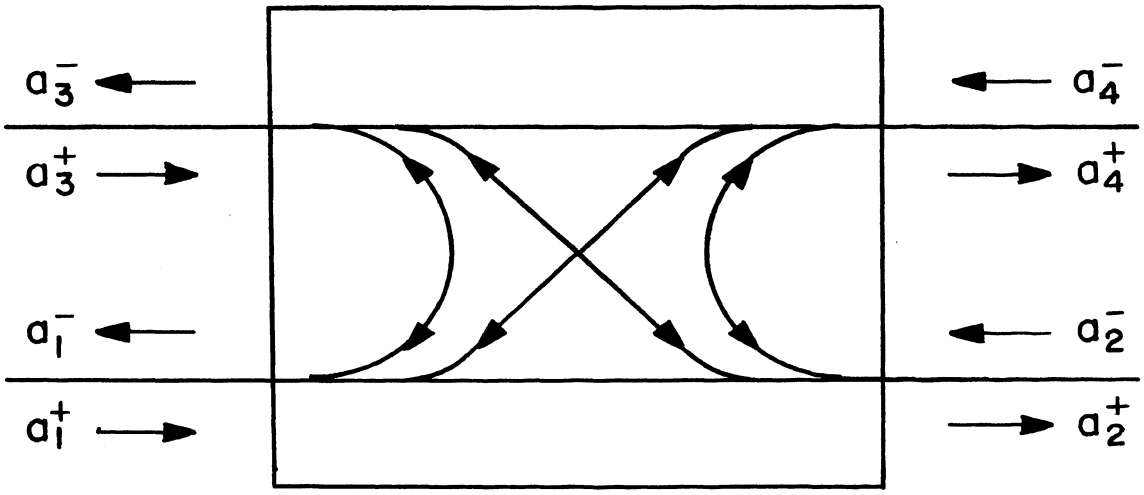

Figure 1. Block Diagram of a Four Port Directional Coupler.

The coupling is defined as

$$C \triangleq \left| \frac{a_3^-}{a_1^+} \right|^2 , \tag{1}$$

or in terms of decibels as

$$C_{db} = 20 \log \left| \frac{a_3^-}{a_1^+} \right| . \tag{2}$$

For microwave use the coupling is normally on the order of -10 or -20db. The directivity, which is a measure of the response of the port which is not coupled, is defined as

$$D \triangleq \left| \frac{a_4^+}{a_3^-} \right|^2 , \tag{3}$$

or in terms of decibels as

$$D_{db} = 20 \log \left| \frac{a_4^+}{a_3^-} \right| . \tag{4}$$

For an ideal coupler with all ports terminated in their characteristic impedance, the directivity is infinite. For practical couplers however, the directivity is on the order of - 20 to -40db.

B. The Model

The model used in this work is a section of two coupled transmission lines where the necessary boundary conditions

are applied to obtain directional coupling. A section of a coupled transmission line may be represented schematically as shown in Figure 2. In this figure the Z's and the Y's represent the series impedance and the shunt admittance of the lines, and the Z_m's and the Y_m's represent the mutual impedance and mutual admittance between the lines. In Figure 2 the conventional notation of using an impedance times a differential element of length has been replaced by simply an impedance since the model is a lumped element model.

A directional coupler can be obtained by considering a small section of the line such as the dashed-in section of Figure 2. This section is reproduced as Figure 3 and is the model used in this work. Couplers corresponding to longer sections of line are obtained by cascading the basic section shown in Figure 3.

C. Single Section Directional Coupler

An equivalent circuit for the model of Figure 3 is shown in Figure 4. In this figure the transformer has been replaced by its equivalent circuit. The terminal voltages and currents are also identified in this figure.

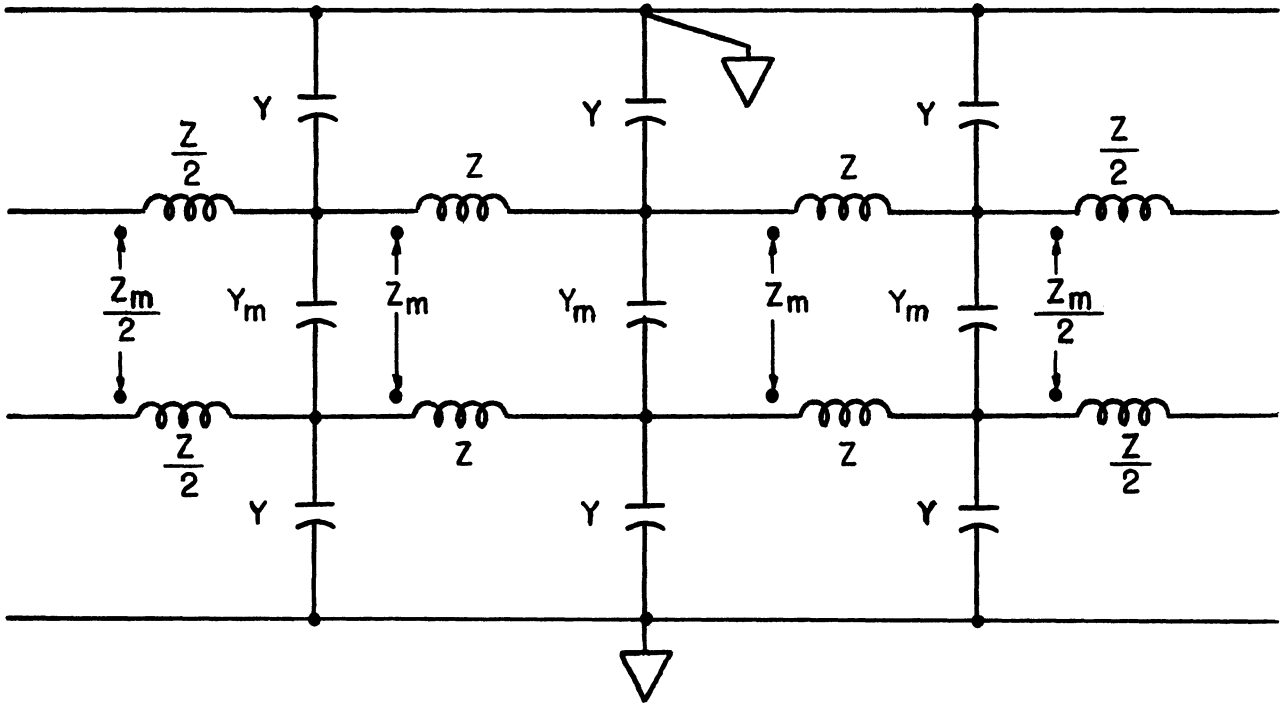

Figure 2. Schematic Representation of a Section of Two Coupled Transmission Lines.

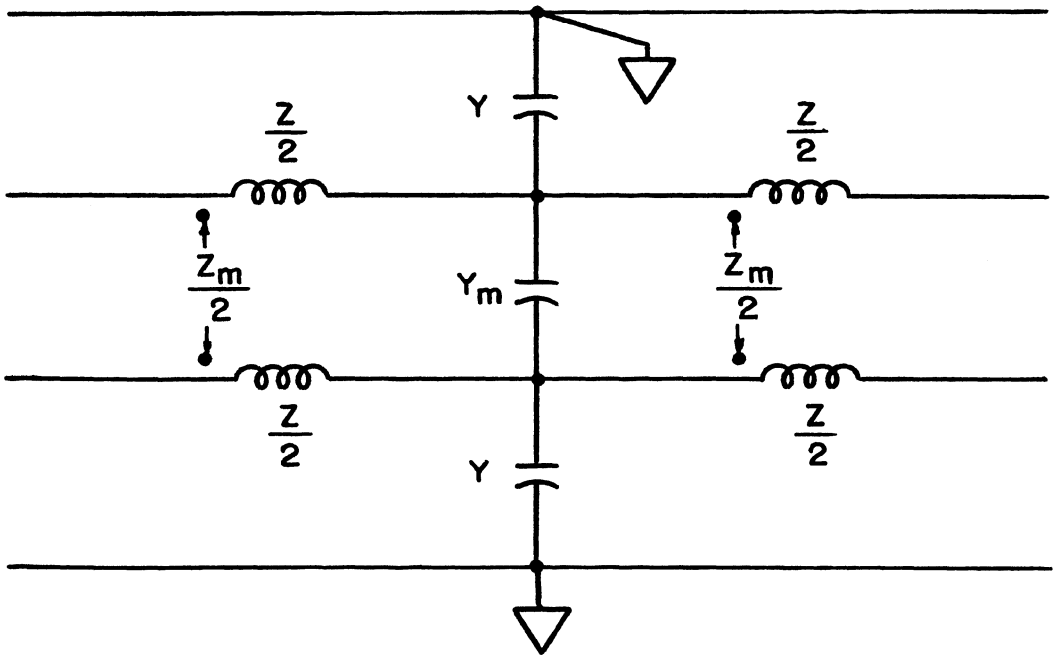

Figure 3. Model for Directional Coupler.

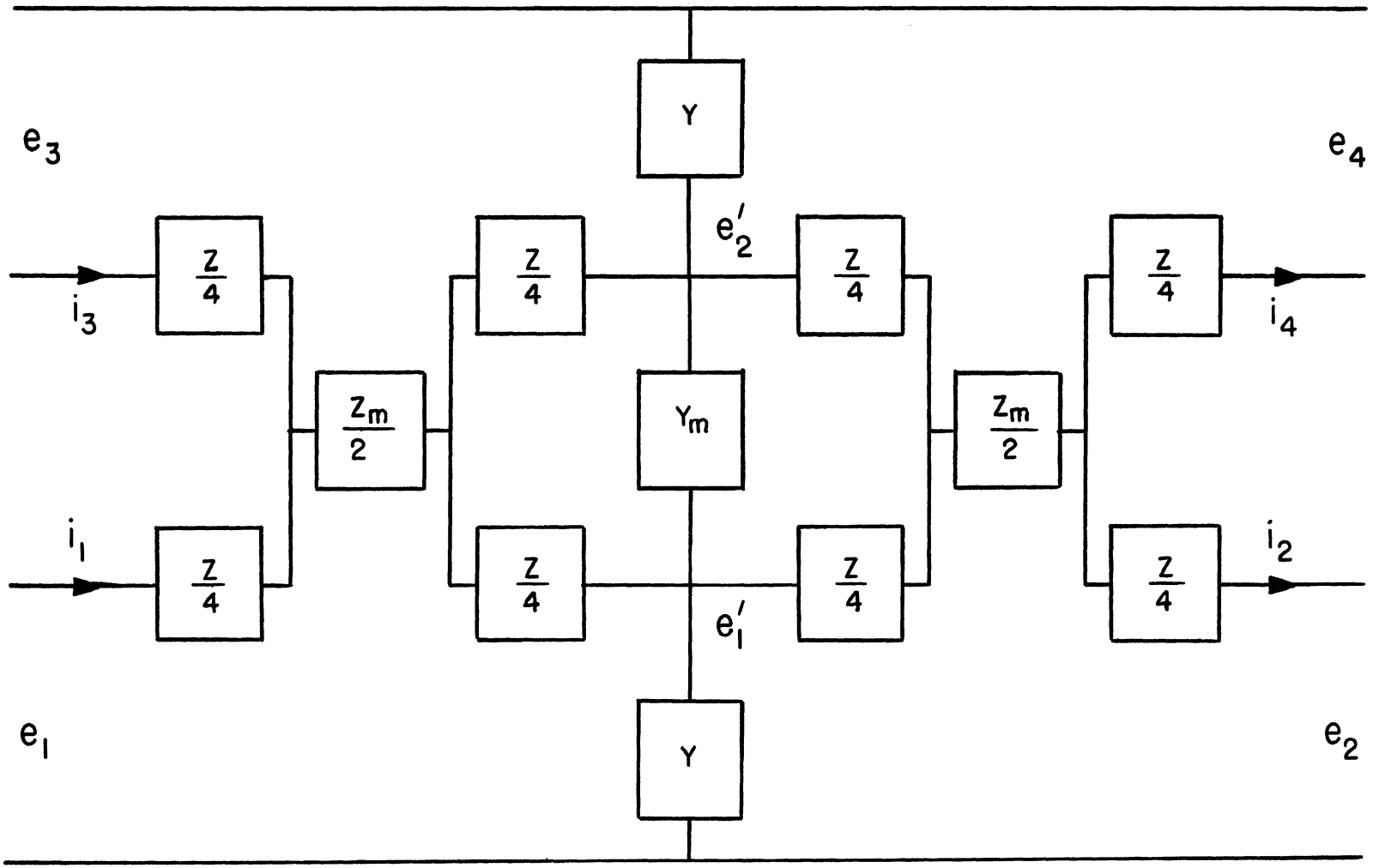

Figure 4. Equivalent Circuit of a Single Section Directional Coupler.

1. General Equations

The voltage-current equations describing this circuit are

$$e_{n1} - e'_1 = \frac{Z+Z_m}{2} i_{n1} + \frac{Z_m}{2} i_{n3} \quad , \tag{5}$$

$$e_{n3} - e'_2 = \frac{Z_m}{2} i_{n1} + \frac{Z+Z_m}{2} i_{n3} \quad , \tag{6}$$

$$e'_1 - e_{n2} = \frac{Z+Z_m}{2} i_{n2} + \frac{Z_m}{2} i_{n4}, \tag{7}$$

$$e'_2 - e_{n4} = \frac{Z_m}{2} i_{n2} + \frac{Z+Z_m}{2} i_{n4} \quad , \tag{8}$$

$$i_{n1} - i_{n2} = (Y + Y_m)\, e'_1 - Y_m\, e'_2 \quad , \tag{9}$$

and

$$i_{n3} - i_{n4} = -Y_m\, e'_1 + (Y + Y_m) e'_1 \quad . \tag{10}$$

e'_1 and e'_2 are eliminated from these equations by solving equations 7 and 8 for e'_1 and e'_2 respectively and substituting these into equations 5, 6, 9, and 10. The resulting equations are

$$e_{n1} - \frac{Z+Z_m}{2} i_{n1} - \frac{Z_m}{2} i_{n3} = e_{n2} + \frac{Z+Z_m}{2} i_{n2} + \frac{Z_m}{2} i_{n4}, \quad (11)$$

$$e_{n3} - \frac{Z_m}{2} i_{n1} - \frac{Z+Z_m}{2} i_{n3} = e_{n4} + \frac{Z_m}{2} i_{n2} + \frac{Z+Z_m}{2} i_{n4}, \quad (12)$$

$$i_{n1} = (Y+Y_m) e_{n2} - Y_m e_{n4} + [1 + \frac{(Y+Y_m)(Z+Z_m)}{2} - \frac{Z_m Y_m}{2}] i_{n2}$$

$$+ [\frac{Z_m(Y+Y_m)}{2} - \frac{Y_m(Z+Z_m)}{2}] i_{n4}, \quad (13)$$

and

$$i_{n3} = - Y_m e_{n2} + (Y+Y_m) e_{n4} + [\frac{Z_m(Y+Y_m)}{2} - \frac{Y_m(Z+Z_m)}{2}] i_{n2}$$

$$+ [1 + \frac{(Y+Y_m)(Z+Z_m)}{2} - \frac{Z_m Y_m}{2}] i_{n4}. \quad (14)$$

Let the following modes be defined[18,19]

$$a^+_{nm} \triangleq \frac{1}{\sqrt{2}} (\frac{e_{nm}}{\sqrt{Z_o}} + \sqrt{Z_o}\, i_{nm}) \quad (15)$$

and

$$a^-_{nm} \triangleq \frac{1}{\sqrt{2}} (\frac{e_{nm}}{\sqrt{Z_o}} - \sqrt{Z_o}\, i_{nm}) \quad (16)$$

where the plus superscript indicates a forward traveling wave and the minus superscript indicates a backward traveling wave. The voltages and currents in terms of the forward and backward traveling waves are obtained by taking the sum and difference of equations 15 and 16. These become

$$e_{nm} = \frac{\sqrt{Z_o}}{\sqrt{2}} (a^+_{nm} + a^-_{nm}) \tag{17}$$

and

$$i_{nm} = \frac{1}{\sqrt{2Z_o}} (a^+_{nm} - a^-_{nm}). \tag{18}$$

Substituting equations 17 and 18 into equations 11 thru 14 and writing equations 11 thru 14 in matrix form, the equation

$$\begin{bmatrix} 1 & 0 & -Z_1 & -Z_2 \\ 0 & 1 & -Z_2 & -Z_1 \\ 0 & 0 & 1 & 0 \\ 0 & 0 & 0 & 1 \end{bmatrix} \begin{bmatrix} a^+_{n1} + a^-_{n1} \\ a^+_{n3} + a^-_{n3} \\ a^+_{n1} - a^-_{n1} \\ a^+_{n3} - a^-_{n3} \end{bmatrix}$$

$$= \begin{bmatrix} 1 & 0 & Z_1 & Z_2 \\ 0 & 1 & Z_2 & Z_1 \\ 2Y_1 & -2Y_2 & Z'_1 & Z'_2 \\ -2Y_2 & 2Y_1 & Z'_2 & Z'_1 \end{bmatrix} \begin{bmatrix} a^+_{n2} + a^-_{n2} \\ a^+_{n4} + a^-_{n4} \\ a^+_{n2} - a^-_{n2} \\ a^+_{n4} - a^-_{n4} \end{bmatrix} \tag{19}$$

is obtained where

$$Z_1 = \frac{Z+Z_m}{2Z_o} , \tag{20}$$

$$Z_2 = \frac{Z_m}{2Z_o} , \tag{21}$$

$$Y_1 = \frac{Z_o(Y+Y_m)}{2} , \tag{22}$$

$$Y_2 = \frac{Z_o Y_m}{2} , \tag{23}$$

$$Z_1' = 1 + 2Z_1Y_1 - 2Z_2Y_2 , \tag{24}$$

and

$$Z_2' = 2(Z_1Y_2 - Z_2Y_1). \tag{25}$$

Equation 19 is written as a transmission matrix by multiplying its right side by the inverse of its left side. This yields

$$\begin{bmatrix} a_{n1}^+ + a_{n1}^- \\ a_{n3}^+ + a_{n3}^- \\ a_{n1}^+ - a_{n1}^- \\ a_{n3}^+ - a_{n3}^- \end{bmatrix} = [T] \begin{bmatrix} a_{n2}^+ + a_{n2}^- \\ a_{n4}^+ + a_{n4}^- \\ a_{n2}^+ - a_{n2}^- \\ a_{n4}^+ - a_{n4}^- \end{bmatrix} \tag{26}$$

where

$$[T] = \begin{bmatrix} Z_1' & -Z_2 & (Z_1+Z_1Z_1'+Z_2Z_2') & (Z_2+Z_2Z_1'+Z_2'Z_1) \\ -Z_2' & Z_1' & (Z_2+Z_2Z_1'+Z_2'Z_1) & (Z_1+Z_1Z_1'+Z_2Z_2') \\ 2Y_1 & -2Y_2 & Z_1' & Z_2' \\ -2Y_2 & 2Y_1 & Z_2' & Z_1' \end{bmatrix} . \quad (27)$$

2. Conditions for Directional Coupling

For contradirectional coupling, the voltage at port one must not be coupled to the voltage at port four. This condition, namely

$$\frac{a_{n1}^{+} + a_{n1}^{-}}{a_{n4}^{+} + a_{n4}^{-}} = 0 \quad (28)$$

requires that

$$Z_2' = 2(Z_1Y_2 - Z_2Y_1) = 0 . \quad (29)$$

This condition, in turn, yields

$$\frac{Z_m}{Z+Z_m} = \frac{Y_m}{Y+Y_m} = k \quad (30)$$

where k is a constant, called the coupling coefficient.

3. Determination of the Characteristic Impedance

If a_{n4}^{-} is the only input ($a_{n1}^{+} = a_{n3}^{+} + a_{n2}^{-} = 0$), a relation between a_{n4}^{-} and a_{n1}^{-} is obtained which leads to an expression for Z_o. Subtracting the third row from the first row of equation 26 and using equation 30, one obtains

$$2\bar{a}_{n1} = [2Y_2 - Z_2(1+Z_1)]\bar{a}_{n4}. \tag{31}$$

But, for directional coupling with no reflections,

$$\frac{\bar{a}_{n1}}{\bar{a}_{n4}} = 0 \ , \tag{32}$$

and

$$2Y_2 - Z_2(1+Z_1) = 0; \tag{33}$$

or

$$Z_o^2 = \frac{Z_m}{Y_m}\left[1 + \frac{(Z+Z_m)(Y+Y_m) - Z_mY_m}{4}\right] \ . \tag{34}$$

An alternate form of Z_o^2 is obtained when equation 30 is used. This yields

$$Z_o^2 = \frac{(Z+Z_m)}{(Y+Y_m)}\left[1 + \frac{(Z+Z_m)(Y+Y_m)(1-k^2)}{4}\right] \ . \tag{35}$$

Substituting equations 29 and 35 into equation 26, the transmission matrix may be written as

$$[T] = \begin{bmatrix} (2\frac{Z_1}{Y_1} - 1) & 0 & 2Y_1 & 2kY_1 \\ 0 & (2\frac{Z_1}{Y_1} - 1) & 2kY_1 & 2Y_1 \\ 2Y_1 & -2kY_1 & (2\frac{Z_1}{Y_1} - 1) & 0 \\ -2kY_1 & 2Y_1 & 0 & (2\frac{Z_1}{Y_1} - 1) \end{bmatrix} \tag{36}$$

in the expression

$$\begin{bmatrix} a_{n1}^{+} + a_{n1}^{-} \\ a_{n3}^{+} + a_{n3}^{-} \\ a_{n1}^{+} - a_{n1}^{-} \\ a_{n3}^{+} - a_{n3}^{-} \end{bmatrix} = [T] \begin{bmatrix} a_{n2}^{+} + a_{n2}^{-} \\ a_{n4}^{+} + a_{n4}^{-} \\ a_{n2}^{+} - a_{n2}^{-} \\ a_{n4}^{+} - a_{n4}^{-} \end{bmatrix} . \qquad (37)$$

4. Scattering Matrix.

In its present form equation 27 shows the relation between the total voltage and current at ports two and four and the total voltage and current at ports one and three. Since interest lies in directional coupling, a more convenient form would be that of a scattering matrix. The scattering matrix shows the relation between the output waves and the input waves.

Equation 37 is easily solved for the output waves in terms of the input waves yielding

$$\begin{bmatrix} a_{n1}^{-} \\ a_{n3}^{-} \\ a_{n2}^{+} \\ a_{n4}^{+} \end{bmatrix} = \frac{\begin{bmatrix} 0 & 2kY_1 & 1 & 0 \\ 2kY_1 & 0 & 0 & 1 \\ 1 & 0 & 0 & 2kY_1 \\ 0 & 1 & 2kY_1 & 0 \end{bmatrix} \begin{bmatrix} a_{n1}^{+} \\ a_{n3}^{+} \\ a_{n2}^{-} \\ a_{n4}^{-} \end{bmatrix}}{2\frac{Y_1}{Z_1} + 2Z_1 + 1} . \qquad (38)$$

The symmetry of the coupler can be seen from this equation by noting that each output term is related to two input terms. One term gives the coupled wave and the other term gives the main feed wave. Note that all the coupling terms are the same and all the main feed wave terms are the same.

Equation 38 may also be written as a transmission matrix. This expression is

$$\begin{bmatrix} a_{n1}^{+} \\ a_{n1}^{-} \\ a_{n3}^{+} \\ a_{n3}^{-} \end{bmatrix} = \begin{bmatrix} -\delta & 0 & 0 & \gamma \\ & -\frac{\gamma^2-1}{\delta} & \gamma & 0 \\ 0 & -\gamma & \delta & 0 \\ -\gamma & 0 & 0 & \frac{\gamma^2-1}{\delta} \end{bmatrix} \begin{bmatrix} a_{n2}^{+} \\ a_{n2}^{-} \\ a_{n4}^{+} \\ a_{n4}^{-} \end{bmatrix} \tag{39}$$

where

$$\delta = 2\frac{Y_1}{Z_1} + 2Z_1 - 1 \tag{40}$$

and

$$\gamma = 2kY_1 \ . \tag{41}$$

The transmission matrix form is more convenient for use in the discussion on cascading two or more sections.

5. Determination of the Cutoff Frequency

The cutoff frequency, ω_o, is obtained from the expression for Z_o^2 (equation 35). At the cutoff frequency Z_o is zero. In the steady state, assuming ideal components, the most likely choice for Z and Y are

$$Z = j\,\omega\,L \tag{42}$$

and

$$Y = j\,\omega\,C \tag{43}$$

therefore, at the cutoff frequency

$$\frac{L + L_m}{C + C_m}\left[1 - \frac{\omega_o^2}{4}(L+L_m)(C+C_m)(1-k^2)\right] = 0. \tag{44}$$

From equation 30,

$$L + L_m = \frac{L}{1-k} \tag{45}$$

and

$$C + C_m = \frac{C}{1-k} \tag{46}$$

so that

$$\omega_o^2 = \frac{4}{LC}\left(\frac{1-k}{1+k}\right) . \tag{47}$$

6. Coupling, Loss and Directivity.

If a_{n1}^+ is the only input, the coupling is given by

$$C = \left|\frac{a_3^-}{a_1^+}\right|^2 = |S_{21}|^2 = \left|\frac{2kY_1}{2\frac{Y_1}{Z_1} + 2Z_1 - 1}\right|^2 \tag{48}$$

or

$$C = \frac{4\left(\frac{\omega}{\omega_o}\right)^2 \left(\frac{k^2}{1-k^2}\right)\left[1 - \left(\frac{\omega}{\omega_o}\right)^2\right]}{1 + 4\left(\frac{\omega}{\omega_o}\right)^2 \left(\frac{k^2}{1-k^2}\right)\left[1 - \left(\frac{\omega}{\omega_o}\right)^2\right]} \quad . \tag{49}$$

The insertion loss is given by

$$G = |S_{31}|^2 = \left| \frac{1}{2\frac{Y_1}{Z_1} + 2Z_1 - 1} \right|^2 \tag{50}$$

or

$$G = \frac{1}{1 + 4\left(\frac{\omega}{\omega_o}\right)^2 \left(\frac{k^2}{1-k^2}\right)\left[1 - \left(\frac{\omega}{\omega_o}\right)^2\right]}. \tag{51}$$

Since the total power out of the coupler must equal the total power into the coupler

$$|S_{11}|^2 + |S_{21}|^2 + |S_{31}|^2 + |S_{41}|^2 = 1, \tag{52}$$

or

$$C + G = 1 \tag{53}$$

since S_{11} and S_{41} are zero. Adding the expressions for C ang G one does indeed obtain unity which indicates the validity of equations 49 and 51.

The directivity is given as

$$D = \left| \frac{S_{14}}{S_{12}} \right|^2 \tag{54}$$

or

$$D_{db} = 20 \log \left| \frac{S_{14}}{S_{12}} \right|$$

and as indicated previously is infinite for the ideal case.

7. Coupling and Bandwidth

It is of interest at this point to examine the bandwidth of the coupler to see what effect the magnitude of the coupling has on the bandwidth and the insertion loss. The bandwidth is defined here as the bandwidth between the half power or 3db points at the coupled port. Figure 5 shows a plot of coupling and insertion loss versus normalized frequency for k^2 values of 0.1, 0.25, and 0.5. The coupling curves show that the bandwidth increases with increasing values of k. The bandwidth is approximately 0.53 ω/ω_o for a k^2 of 0.1 and approximately 0.61 ω/ω_o for a k^2 of 0.5. For k^2 greater than 0.5, the loss will fall below the half power point, thus restricting the bandwidth to much smaller values. The k^2 equal 0.5 coupler is a 3db coupler or power splitter.

8. Coupler Design

To be able to construct a lumped element coupler it is necessary to have a means of determining the component values necessary to produce a given coupling for a given characteristic impedance and cutoff frequency. In the procedure that follows it is assumed that the characteristic impedance, the cutoff frequency, and the maximum coupling, in decibels, are known.

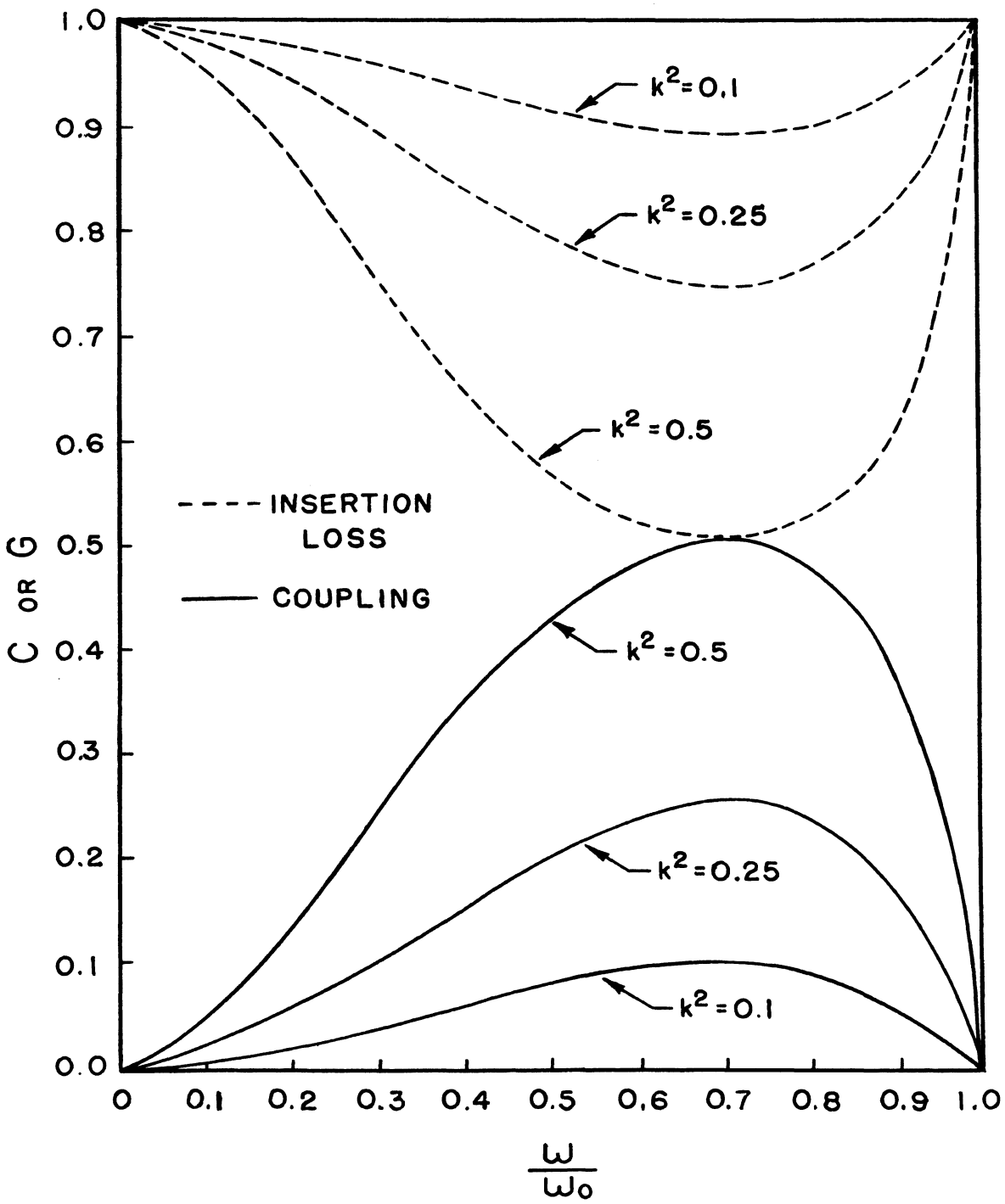

Figure 5. Coupling and Insertion Loss Versus Normalized Frequency for a Single Section Coupler With k Varied as a Parameter.

The value of the coupling coefficient, k, is determined from equation 49 and the fact that maximum coupling occurs at $\omega/\omega_o = 0.707$. When equation 49 is solved with this value of ω/ω_o one obtains

$$k = (C_{max})^{1/2} \tag{56}$$

or when C is in decibels

$$k = 10^{-\frac{C_{max}}{20}} \tag{57}$$

where C is positive.

At low frequencies, equation 44 can be approximated by

$$Z_o^2 \simeq \frac{L}{C} \quad , \tag{58}$$

or

$$C = \frac{L}{Z_o^2} \quad . \tag{59}$$

The cutoff frequency is given by

$$\omega_o^2 = \frac{4Z_o^2(1-k)}{L^2(1+k)} \tag{60}$$

where equation 59 has been substituted for C. L is therefore given by

$$L = \frac{2Z_o}{\omega_o} \left(\frac{1-k}{1+k}\right)^{1/2} \tag{61}$$

and C is now obtained from equation 59. From equation 30, L_m and C_m are

$$L_m = \frac{k}{1-k} L \tag{62}$$

and

$$C_m = \frac{k}{1-k} C \tag{63}$$

Equations 57, 59, 61, 62, and 63 gives the desired component values.

9. Matching Network

In practical applications, it is necessary that the input impedance at each port of the coupler remain constant over the desired frequency range. Z_o, however, is not constant but varies considerably with frequency which can be seen when Z_o is written as

$$Z_o = \{\frac{L}{C}[1 - (\frac{\omega}{\omega_o})^2]\}^{1/2}. \tag{64}$$

A plot of Z_o, normalized to its low frequency value of L/C, versus normalized frequency is shown in Figure 6. When written as

$$Z_o = [\frac{Z+Z_m}{Y+Y_m} + \frac{(Z+Z_m)^2(1-k^2)}{4}]^{1/2} \tag{65}$$

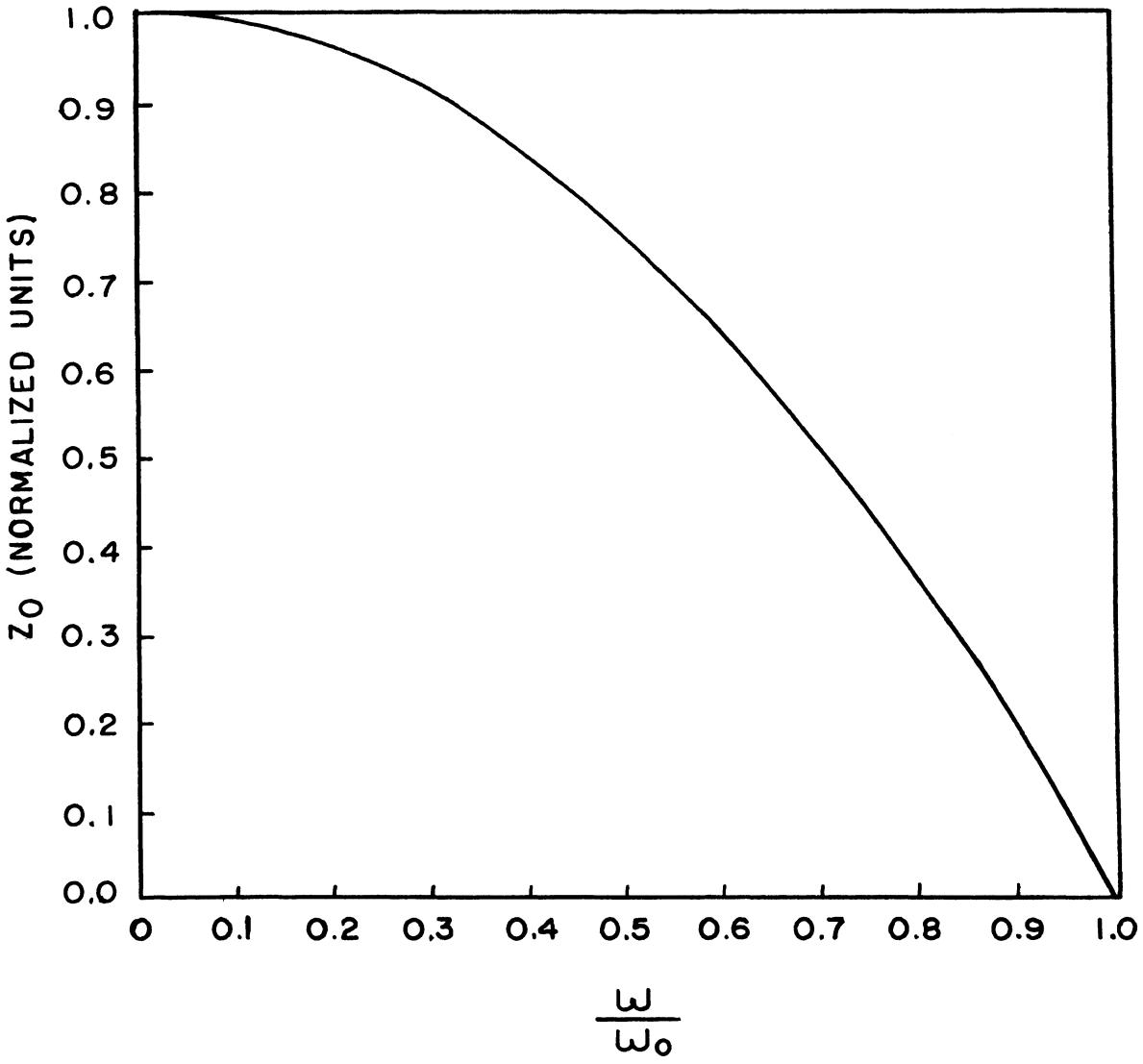

Figure 6. Normalized Z_o Versus Normalized Frequency.

the characteristic impedance has the form

$$Z_o = [Z_{T1}Z_{T2} + \frac{Z_{T1}^2}{2}]^{1/2} \tag{66}$$

where

$$Z_{T1} = (Z+Z_m)(1-k^2)^{1/2} \tag{67}$$

and

$$Z_{T2} = \frac{1}{(Y+Y_m)(1-k^2)^{1/2}} \quad . \tag{68}$$

Equation 66 is the same as the input impedance of a single section "Tee" type ladder network. For purposes of matching, then, each port of the coupler is considered to be the input of a single "Tee" type ladder network.

Z_o can be matched to a constant impedance line by using a matching network of the series m-derived type[20]. The low pass prototype of this filter is the single section "Tee" type previously discussed. The prototype and two m-derived half sections are shown in Figure 7. The component values to be used in the half sections are

$$L_A = \frac{m}{2}(L+L_m)(1-k^2)^{1/2} \quad , \tag{69}$$

$$L_B = \frac{1-m^2}{2m}(L+L_m)(1-k^2)^{1/2} \quad , \tag{70}$$

and

$$C_c = \frac{2}{m(C+C_m)(1-k^2)^{1/2}} \tag{71}$$

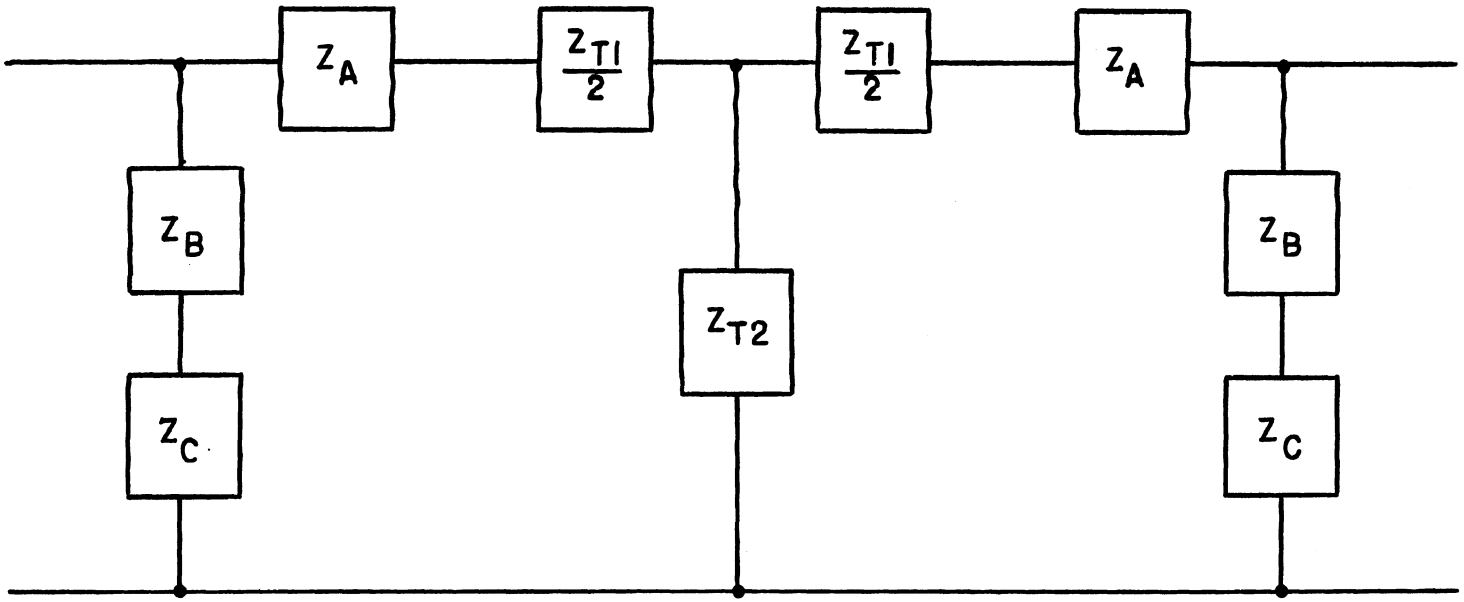

Figure 7. Matching Network With Low Pass Prototype.

where m is a parameter which determines the variations in the input impedance of the matching network. Minimum variation in the impedance occurs when m is 0.6. This value of m produces a 4 percent variation in the impedance over 90 percent of the pass band.

D. Two Section Directional Coupler

A two section directional coupler is obtained by cascading two single section couplers as shown in Figure 8. The two sections need not be identical provided their impedances are matched[19].

1. Condition for Cascading Sections

When two sections are cascaded their input impedances must be matched in order to maintain infinite directivity in the ideal case. Any mismatch will produce reflections at the mismatch which will result in reduced directivity and increased insertion loss. For the impedance of the two sections to be matched,

$$Z_{o1} = Z_{o2} \tag{72}$$

or

$$\frac{L_1}{C_1}\left[1 - \omega^2 L_1 C_1 \frac{(1-k_1)}{(1+k_1)}\right] = \frac{L_2}{C_2}\left[1 - \omega^2 L_2 C_2 \frac{(1-k_2)}{(1+k_2)}\right] . \tag{73}$$

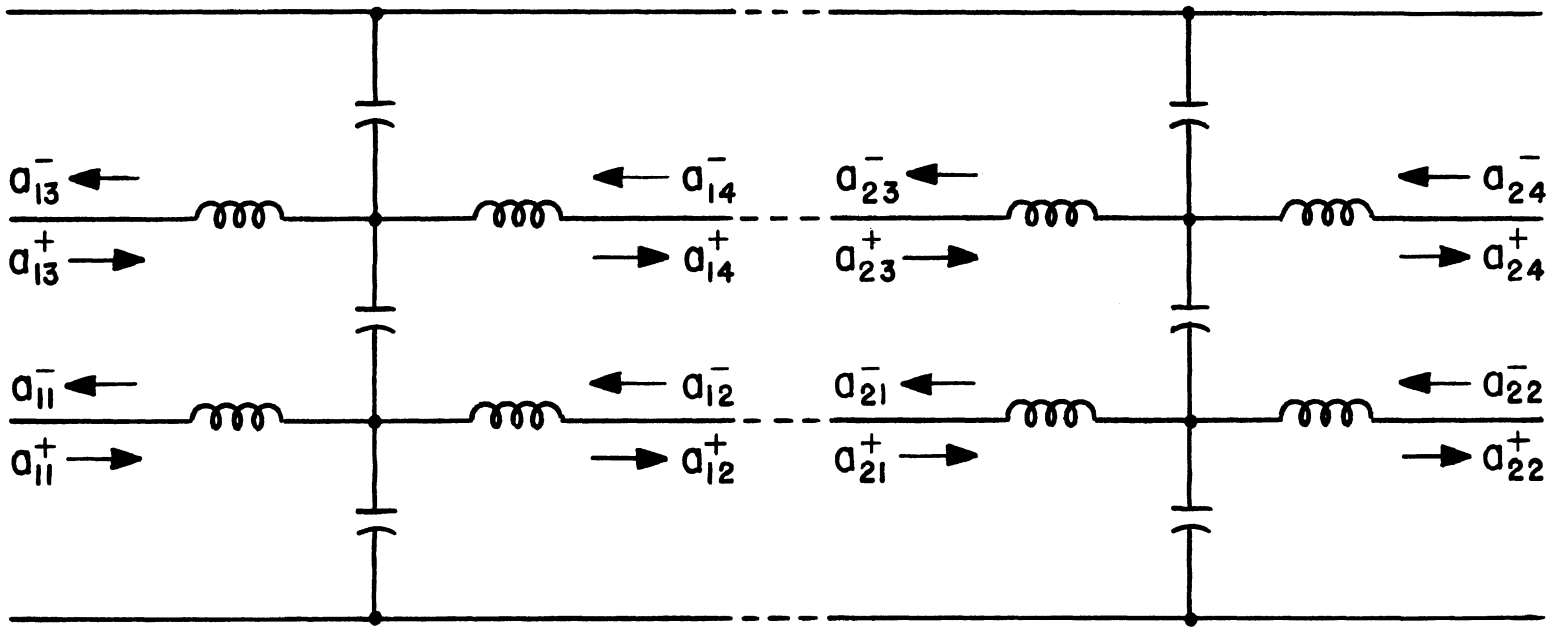

Figure 8. Schematic Representation of a Two Section Directional Coupler.

This condition requires that

$$\frac{L_1}{C_1} = \frac{L_2}{C_2} \tag{74}$$

and

$$L_1^2\frac{(1-k_1)}{(1+k_1)} = L_2^2\frac{(1-k_2)}{(1+k_2)} \quad . \tag{75}$$

L_2 and C_2 are therefore given as

$$L_2 = L_1 \left[\frac{(1-k_1)(1+k_2)}{(1+k_1)(1-k_2)}\right]^{1/2} \tag{76}$$

and

$$C_2 = \frac{C_1 L_2}{L_1} \tag{77}$$

2. General Equations

The equations for a two section coupler are derived by writing a transmission matrix for each of the two sections and then multiplying the two matrices together. The transmission matrix for a single section coupler is given by equation 39.

At this point it is convenient to write the elements of the transmission matrix in terms of complex quantities. From their definitions,

$$\delta_n = \left[1-2\left(\frac{\omega}{\omega_o}\right)^2\right] + j\,\frac{2}{1-k_n}\left(\frac{\omega}{\omega_o}\right)\left\{\frac{1-k_n}{1+k_n}\left[1 - \left(\frac{\omega}{\omega_o}\right)^2\right]\right\}^{1/2} \tag{78}$$

and

$$\gamma_n \triangleq j\frac{2k_n}{1-k_n}\left(\frac{\omega}{\omega_o}\right)\left\{\frac{1-k_n}{1+k_n}\left[1-\left(\frac{\omega}{\omega_o}\right)^2\right]\right\}^{1/2} . \tag{79}$$

Now define

$$\rho \triangleq 1 - 2\left(\frac{\omega}{\omega_o}\right)^2 \tag{80}$$

and

$$\sigma_n \triangleq \frac{2}{1-k_n}\left(\frac{\omega}{\omega_o}\right)\left\{\frac{1-k_n}{1+k_n}\left[1-\left(\frac{\omega}{\omega_o}\right)^2\right]\right\}^{1/2} \tag{81}$$

so that

$$\delta_n = \rho + j\,\sigma_n \tag{82}$$

and

$$\gamma_n = j\,k_n\,\sigma_n . \tag{83}$$

The transmission matrix may now be written as

$$[T_n] = \begin{bmatrix} -(\rho+j\sigma_n) & 0 & 0 & jk_n\sigma_n \\ 0 & \frac{k_n^2\sigma_n^2+1}{\rho+j\sigma_n} & jk_n\sigma_n & 0 \\ 0 & -jk_n\sigma_n & \rho+j\sigma_n & 0 \\ -jk_n\sigma_n & 0 & 0 & -\left(\frac{k_n^2\sigma_n^2+1}{\rho+j\rho_n}\right) \end{bmatrix} . \tag{84}$$

The transmission matrix for the two section coupler is

$$\begin{bmatrix} a_{11}^{+} \\ a_{11}^{-} \\ a_{13}^{+} \\ a_{13}^{-} \end{bmatrix} = [T_1]\ [T_2] \begin{bmatrix} a_{22}^{+} \\ a_{22}^{-} \\ a_{24}^{+} \\ a_{24}^{-} \end{bmatrix} \tag{85}$$

where T_1 and T_2 are defined by equation 84. Carrying out the indicated multiplication, one obtains

$$\begin{bmatrix} a_{11}^{+} \\ a_{11}^{-} \\ a_{13}^{+} \\ a_{13}^{-} \end{bmatrix} = \begin{bmatrix} F_1 & 0 & 0 & F_4 \\ 0 & F_3 & F_2 & 0 \\ 0 & F_4 & F_4 & 0 \\ F_2 & 0 & 0 & F_3 \end{bmatrix} \begin{bmatrix} a_{22}^{+} \\ a_{22}^{-} \\ a_{24}^{+} \\ a_{24}^{-} \end{bmatrix} \tag{86}$$

where

$$F_1 = (\rho+j\sigma_1)(\rho+j\sigma_2) + k_1k_2\sigma_1\sigma_2 \quad , \tag{87}$$

$$F_2 = j\ k_1\sigma_1(\rho+j\sigma_2) + j\ \frac{k_2\sigma_2(k_1^2\sigma_1^2+1)}{(\rho+j\sigma_1)} \quad , \tag{88}$$

$$F_3 = \frac{(k_1^2\sigma_1^2+1)(k_2^2\sigma_2^2+1)}{(\rho+j\sigma_1)(\rho+j\sigma_2)} + k_1k_2\sigma_1\sigma_2 \quad , \tag{89}$$

and

$$F_4 = -jk_2\sigma_2(\rho+j\sigma_1)-j\frac{k_1\sigma_1(k_2^2\sigma_2^2+1)}{(\rho+j\sigma_2)} \quad . \tag{90}$$

3. Scattering Matrix

The scattering matrix for the two section coupler is obtained by solving equation 86 for the output waves in terms of the input waves. The resulting scattering matrix is

$$\begin{bmatrix} a_{11}^- \\ a_{13}^- \\ a_{22}^+ \\ a_{24}^+ \end{bmatrix} = \begin{bmatrix} 0 & \frac{F_2}{F_1} & \frac{F_1F_3-F_2F_4}{F_1} & 0 \\ \frac{F_2}{F_1} & 0 & 0 & \frac{F_1F_3-F_2F_4}{F_1} \\ \frac{1}{F_1} & 0 & 0 & -\frac{F_4}{F_1} \\ 0 & \frac{1}{F_1} & -\frac{F_4}{F_1} & 0 \end{bmatrix} \begin{bmatrix} a_{11}^+ \\ a_{13}^+ \\ a_{22}^- \\ a_{24}^- \end{bmatrix} \quad . \tag{91}$$

If a_{11}^+ is the only input, the ratio of the coupled wave to the input wave is

$$\frac{a_{13}^-}{a_{11}^+} = \frac{F_2}{F_1} \tag{92}$$

and the ratio of the main output wave to the input wave is

$$\frac{a_{22}^+}{a_{11}^+} = \frac{1}{F_1} \quad . \tag{93}$$

4. Coupling and Insertion Loss

The coupling is

$$C = \left|S_{21}\right|^2 \tag{94}$$

or

$$C = \left| \frac{jk_1\sigma_1(\rho+j\sigma_1)(\rho+j\sigma_2) + k_2\sigma_2(k_1^2\sigma_1^2+1)}{(\rho+j\sigma_1)[(\rho+j\sigma_1)(\rho+j\sigma_2)+k_1k_2\sigma_1\sigma_2]} \right|^2 . \tag{95}$$

Taking the square of the magnitude of this expression, one obtains

$$C = \frac{1}{\rho^2+\sigma_1^2} \left\{ \frac{[k_1\rho^2\sigma_1 - k_1(1-k_1k_2)\sigma_1^2\sigma_2 + k_2\sigma_2]^2 + k_1^2\rho^2\sigma_1^2(\sigma_1+\sigma_2)^2}{[\rho^2-(1-k_1k_2)\sigma_1\sigma_2]^2 + \rho^2(\sigma_1+\sigma_2)^2} \right\} . \tag{96}$$

The coupling is then written as the ratio of polynomials in ρ as

$$C = \left[\frac{F_4\rho^4 + F_2\rho^2 + F_o}{G_4\rho^4 + G_2\rho^2 + G_o} \right] \tag{97}$$

where

$$F_4 = -2k_1k_2[1-k_1k_2 + (1-k_1^2)^{1/2}(1-k_2^2)^{1/2}], \tag{98}$$

$$F_2 = 2k_1k_2[2-k_1k_2+(1-k_1^2)^{1/2}(1-k_2^2)^{1/2}]-(k_1^2+k_2^2) \tag{99}$$

$$F_o = (k_1-k_2)^2, \tag{100}$$

$$G_4 = F_4 , \tag{101}$$

$$G_2 = 2k_1k_2[1-k_1k_2+(1-k_1^2)^{1/2}(1-k_2^2)^{1/2}]-(k_1^2-k_2^2), \tag{102}$$

and

$$G_o = (1-k_1k_2)^2 . \tag{103}$$

The insertion loss is

$$G = |S_{31}|^2 \tag{104}$$

or

$$G = \left| \frac{1}{(\rho+j\sigma_1)(\rho+j\sigma_2) + k_1k_2\sigma_1\sigma_2} \right|^2 . \tag{105}$$

Taking the square of the magnitude of this expression, the insertion loss becomes

$$G = \frac{(1-k_1^2)(1-k_2^2)}{G_4\rho^4+G_2\rho^2+G_o} . \tag{106}$$

5. Two Sections With Identical k's

A special case of the two section coupler arises when both sections have the same coupling coefficient. In this case the expressions for the coupling and the insertion loss are considerably simplified. When $k_1 = k_2$, the coupling is

$$C = \frac{k^2(1-\rho^2)}{1-k^2\rho^2} \left[\frac{4\rho^2(1-k^2\rho^2)}{4k^2\rho^2(1-\rho^2)+(1-k^2)}\right] \tag{107}$$

where the term outside the bracket is the coupling for a single section. The insertion loss for $k_1 = k_2$ is

$$G = \frac{(1-k^2)}{4k^2\rho^2(1-\rho^2)+(1-k^2)} \quad . \tag{108}$$

Adding the expressions for C and G one obtains

$$C + G = 1 \tag{109}$$

as they must for the ideal case.

Figure 9 shows a plot of coupling versus normalized frequency for k = 0.316. The fact that the coupling goes to zero at $\omega/\omega_o = 0.707$ is expected and is due to the term $\rho = 1 - 2(\omega/\omega_o)^2$ in the numerator.

6. Two Sections With Different k's

The notch in the coupling at $\omega/\omega_o = 0.707$ can be removed by using two sections having different coupling coefficients. The general expression for the coupling is given by equation 97. Figure 10 shows plot of the coupling versus normalized frequency with k_1 fixed and k_2 varied as a parameter. This figure shows that as k_2 is made smaller with respect to k_1 the dip in the coupling decreases and the coupling becomes more uniform over the frequency range. The same kind of results would be obtained if k_1 and k_2 are interchanged in equation 97.

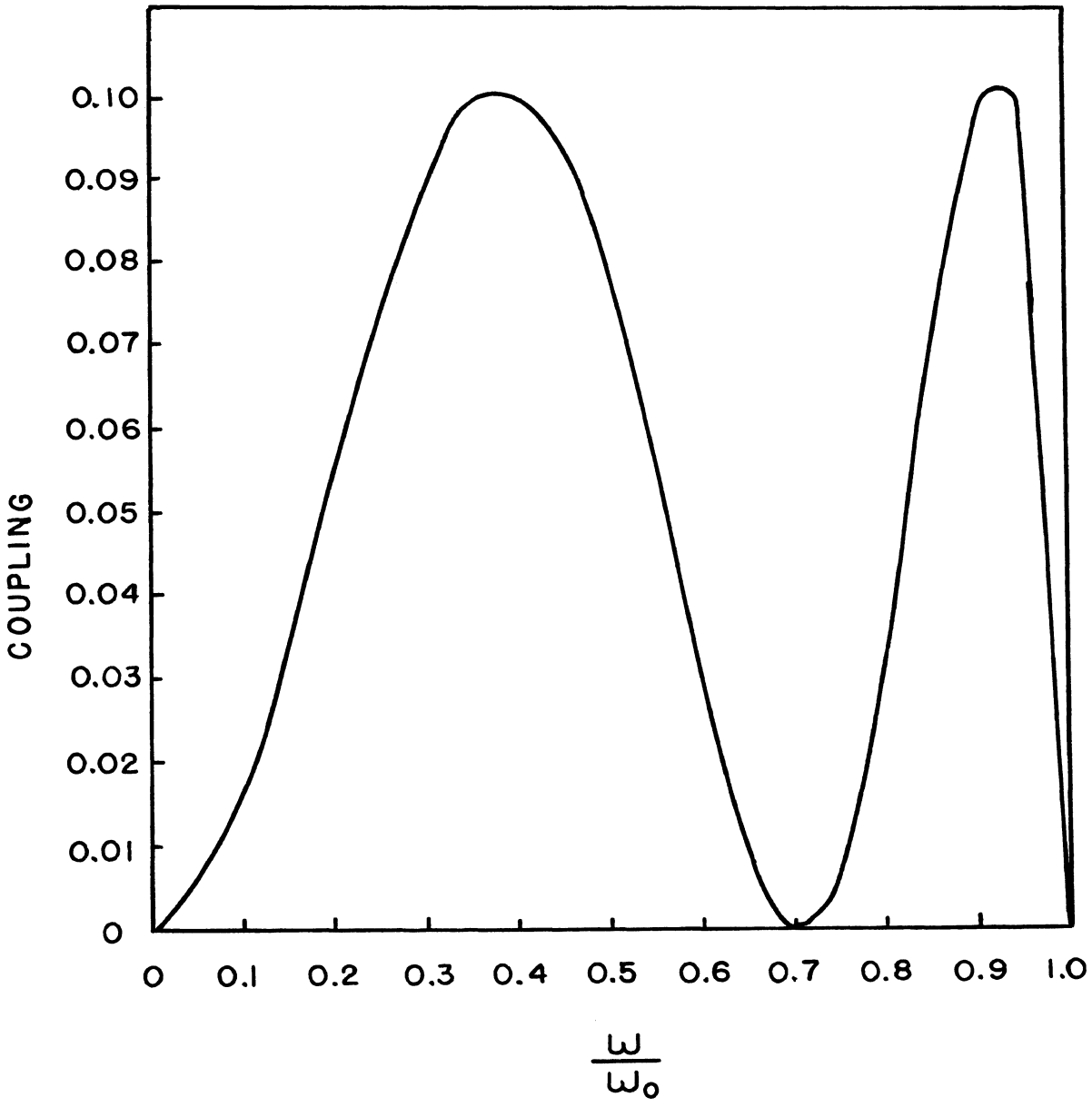

Figure 9. Coupling Versus Normalized Frequency for a Two Section Coupler With $k_1=k_2=0.316$.

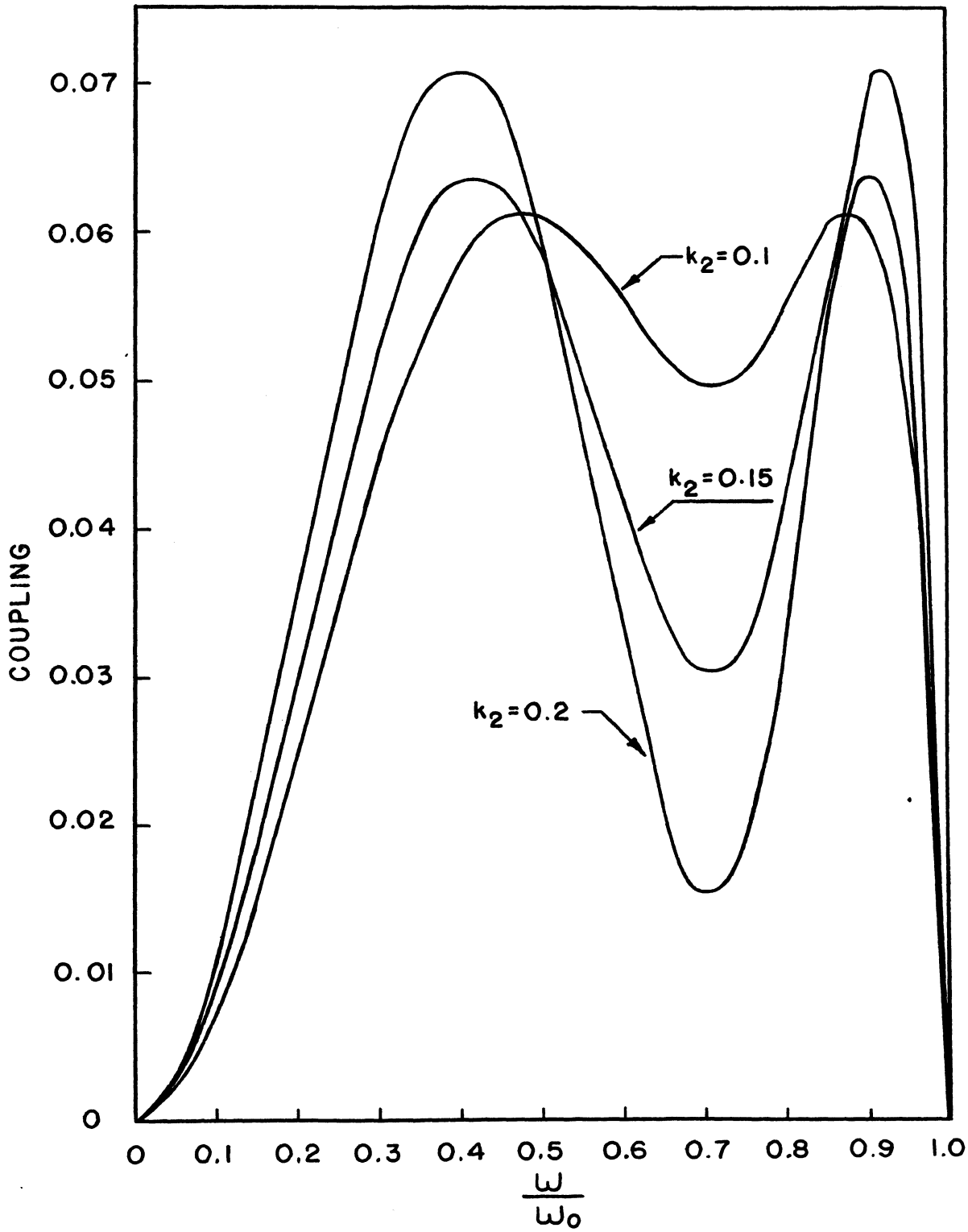

Figure 10. Coupling Versus Normalized Frequency for a Two Section Coupler With k_1=0.316 and k_2 Varied as a Parameter.

Comparison of Figure 10 with Figure 5 shows that the bandwidth of the two section coupler is increased over that of the single section coupler. The maximum 3db bandwidth shown for the two section coupler is 0.74 ω/ω_o as compared to 0.53 ω/ω_o for the single section coupler with similar coupling.

E. Three Section Directional Coupler

A three section directional coupler can be constructed using the procedure outlined in the previous section. Again, the impedance of the sections that are cascaded must be matched in order to maintain high directivity. This requires that

$$\frac{L_1}{C_1} = \frac{L_2}{C_2} = \frac{L_3}{C_3} \tag{110}$$

and

$$L_1^2 \frac{(1-k_1)}{(1+k_1)} = L_2^2 \frac{(1-k_2)}{(1+k_2)} = L_3^2 \frac{(1-k_2)}{(1+k_3)} \tag{111}$$

The equations for three section couplers are derived in the same manner as for the two section coupler. That is, write a transmission matrix for each section and then multiply the matrices. The resulting matrix is then solved for the output waves in terms of the input waves to obtain the scattering matrix.

The elements of the transmission and scattering matrices are extremely complex and do not lend themselves to easy manipulation, even for the simplest case of identical coupling coefficients. The coupling can be obtained for specific values of the coupling coefficient by computer solution. The results shown below were obtained by computer using the values of the coupling coefficients indicated.

Figure 11 shows a plot of coupling versus normalized frequency for three section coupler having identical coupling coefficients. The coupling is now seen to exhibit two notches. This would suggest that for N cascaded sections there are N-1 notches in the coupling.

The shape of the coupling curve can be changed, as before, by using sections with different coupling coefficients. Figure 12 shows a plot of coupling versus frequency for $k_2 = 0.316$ and various values of $k_1 = k_3$. Note that as $k_1 = k_3$ is made smaller the two merge into a single dip. The depth of the dip decreases as $k_1 = k_3$ becomes smaller. The shape of the coupling curve also approaches that of the two section coupler for small k_1.

To study the three section coupler further it would be necessary to obtain the expression for the coupling

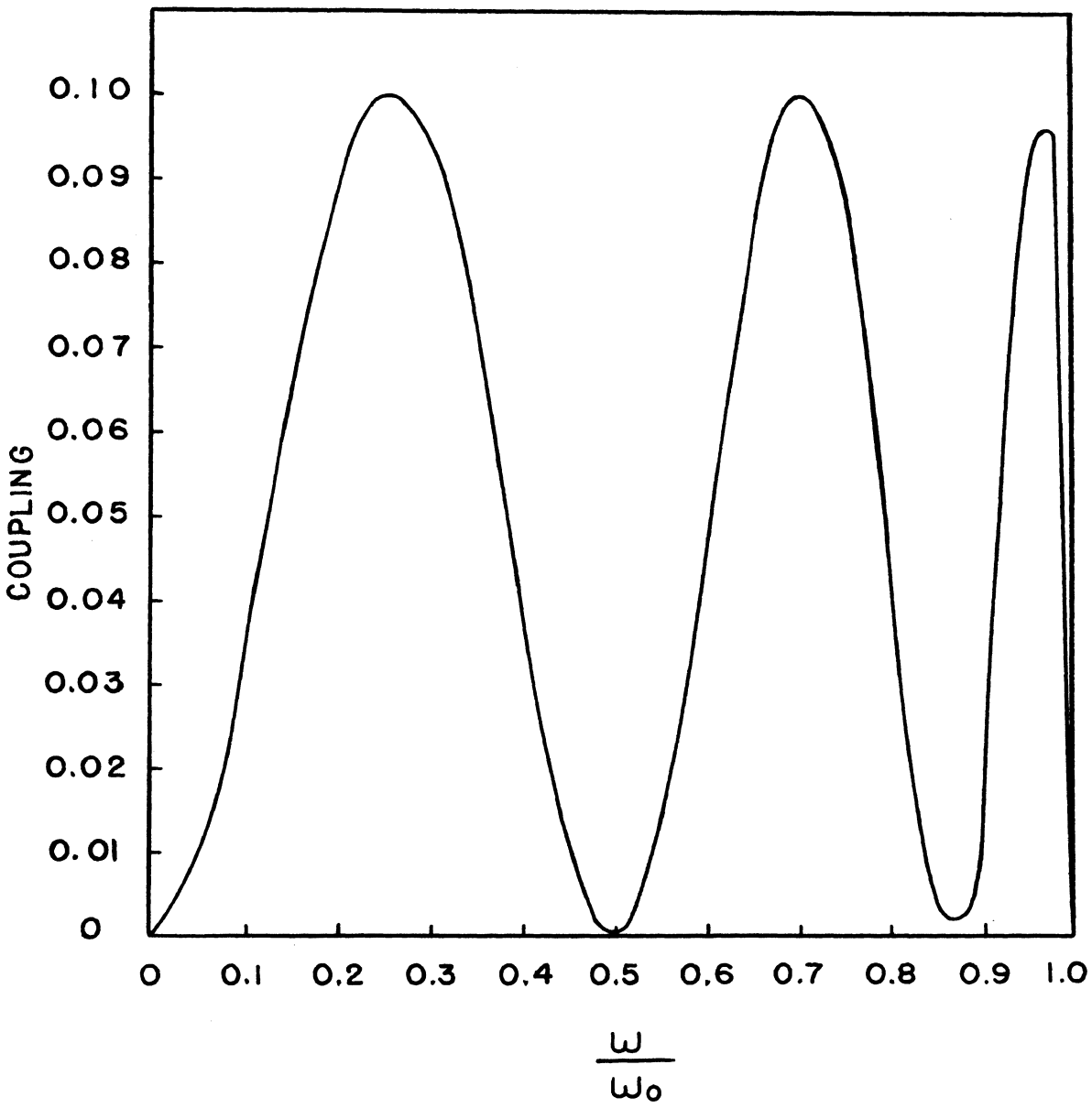

Figure 11. Coupling Versus Normalized Frequency for a Three Section Coupler with $k_1=k_2=k_3=0.316$.

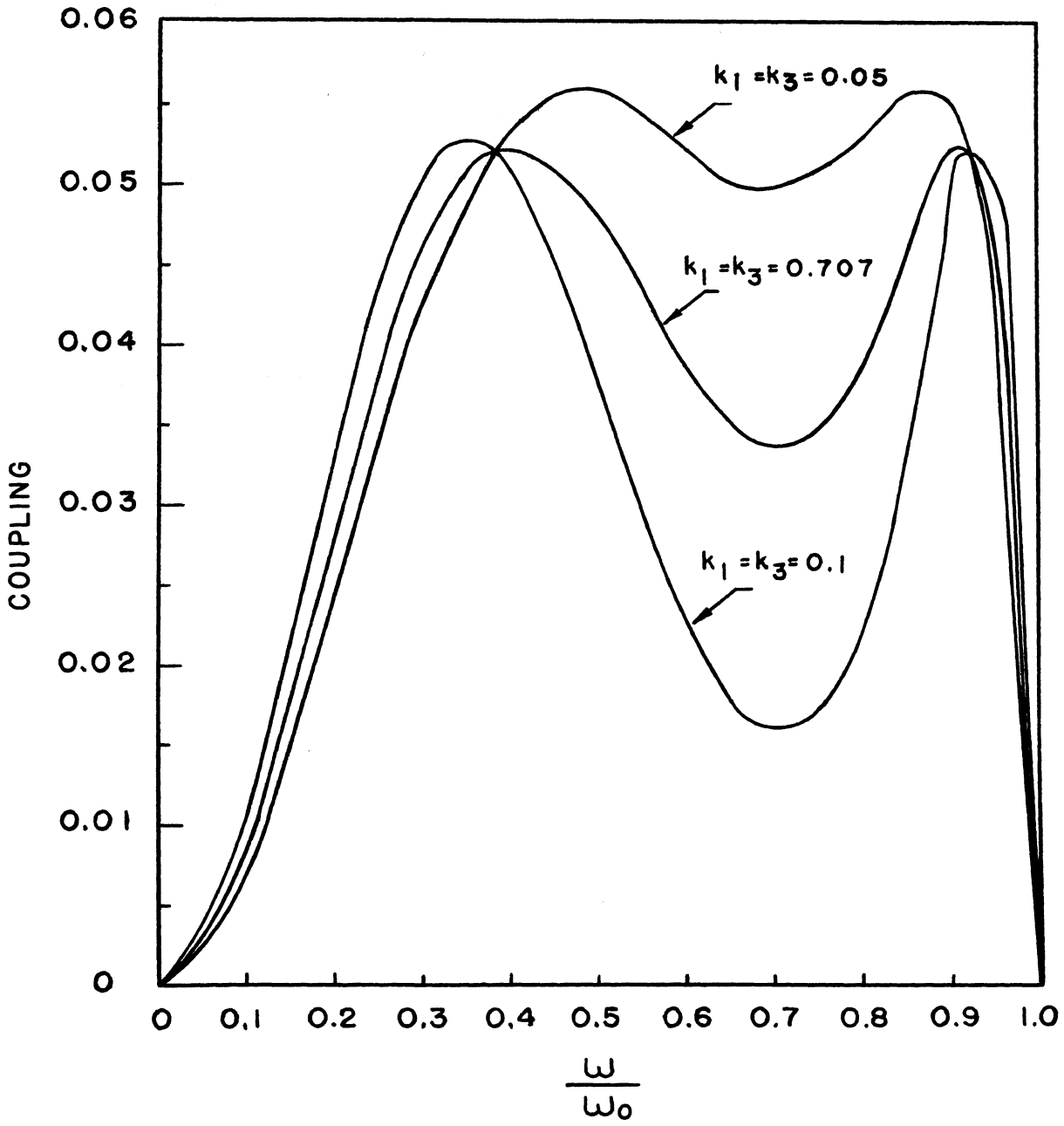

Figure 12. Coupling Versus Normalized Frequency for a Three Section Coupler With $k_2=0.316$ and $k_1=k_3$ Varied as a Parameter.

in terms of the coupling coefficients. It would then be necessary to maximize this expression with respect to bandwidth or to minimize it with respect to variations in coupling. This procedure is beyond the scope of this work.

F. Experimental Procedure

To test the validity of the model, lumped element couplers having one, two, and three sections were constructed and tested. The transformers were wound on 5/16 in. fiber cores with 13 turns of 21 gauge enameled copper wire per winding. The number of turns and the spacing between windings were determined experimentally. Due to the small number of turns involved, difficulties in obtaining the proper coupling and self-inductance were encountered. Any small change in the winding, such as a loose turn or a small bend in the wire, would change the coupling, or the self inductance, or both. Each transformer was hand wound and then measured. If its measured valves were not correct, it had to be rewound and remeasured until the proper values were obtained. Because of the difficulties in constructing the transformers, the tests of the multisection couplers were limited to those with identical sections. The couplers were designed to have a maximum coupling of 10db, a cutoff frequency of 10MHz, and a characteristic impedance of 50 ohms. The tests were

run with all ports terminated in 50 ohm resistive loads. Figure 13 is a schematic representation of the single section coupler with its matching networks. Figure 14 shows a photograph of the prototype. The component values shown were calculated using the procedure outlined previously. The two and three section couplers have additional one and two sections, respectively, added to the diagram shown.

A Wavetek model 142 signal generator was used as a source and held constant at one volt rms. Output voltages were measured with a Hewlett-Packard model 3400B rms voltmeter. Figure 14 shows the test setup used in all measurements. The voltmeter shown connected to port four was also used to measure the voltages at ports two and three.

G. Experimental Results

The three couplers discussed in the preceeding section were tested over their full frequency range. Figure 15 is a plot of the coupling, directivity, and insertion loss versus frequency for the single section coupler. The dashed line in this figure is the coupling calculated from theory. Measured values of coupling are seen to be in close agreement with the calculated values. The coupling decreases faster near the cutoff frequency than is predicted. This is most probably due to resistance losses in the coupler and matching network which were assumed to be zero in the theoretical development. There is also some

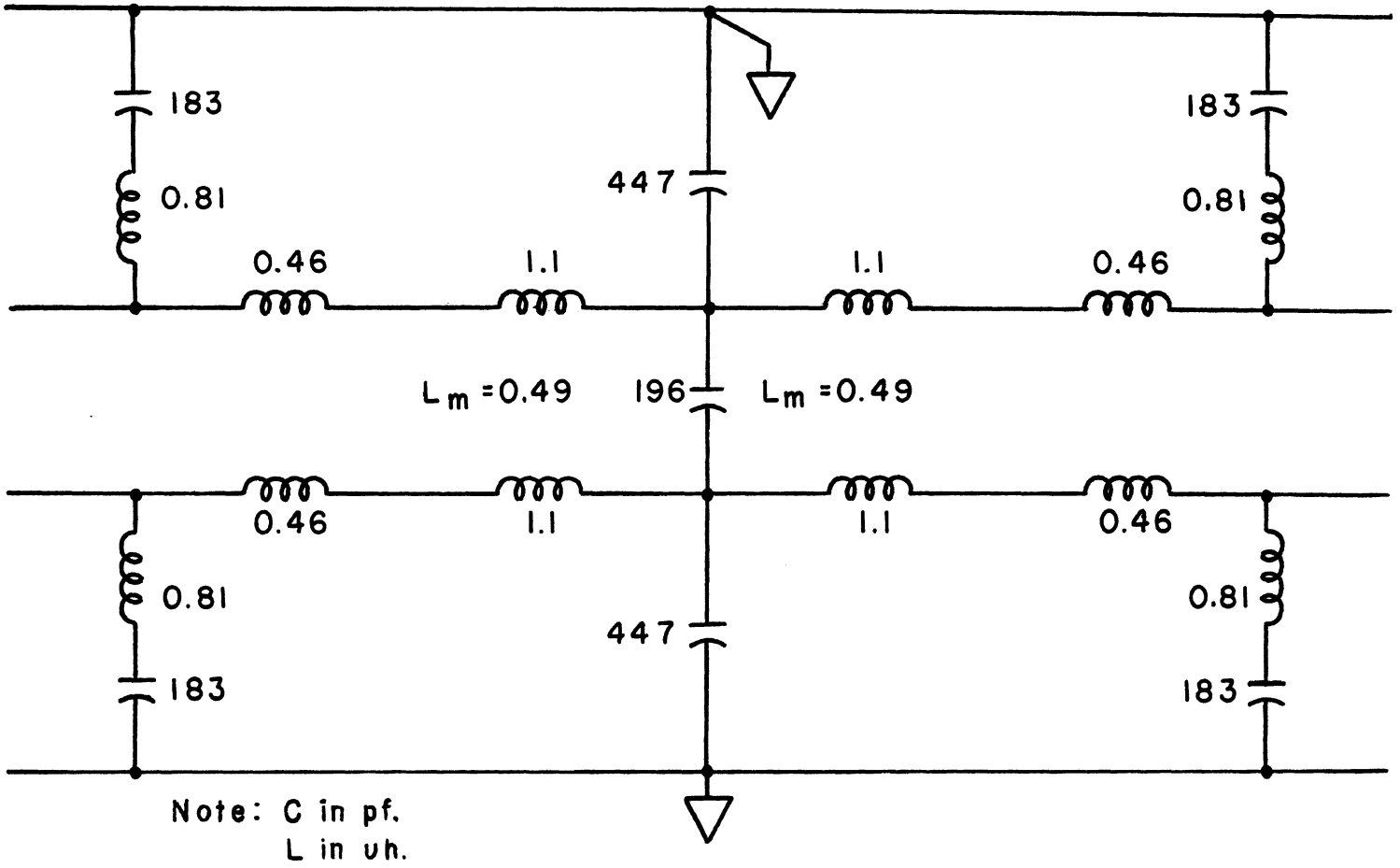

Figure 13. Schematic Representation of a Single Section Coupler and its Matching Network.

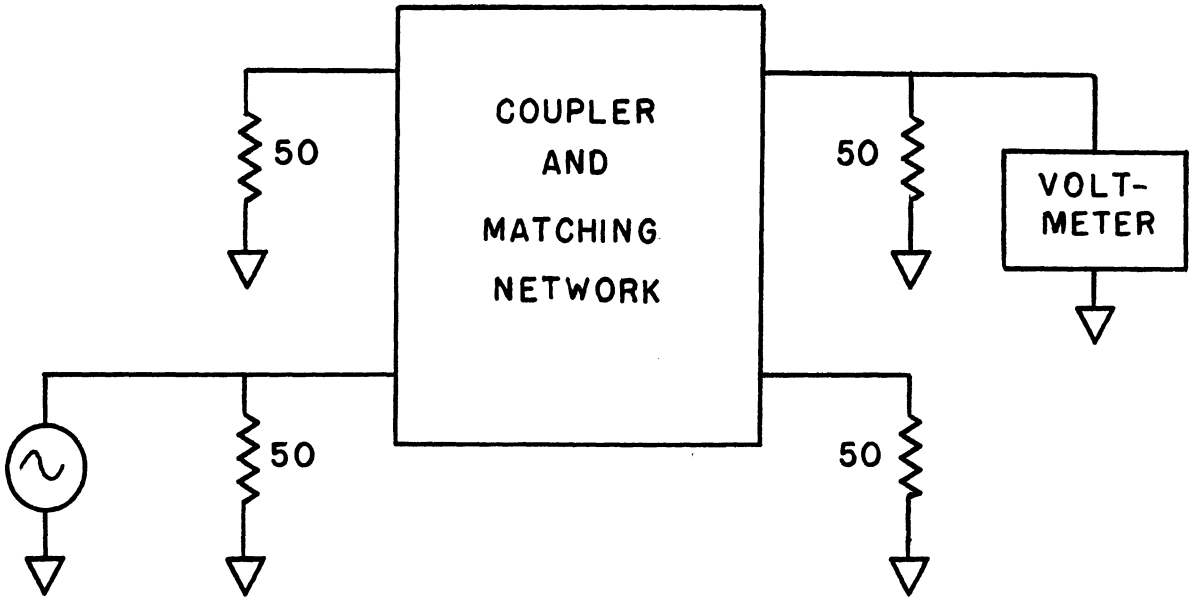

Figure 14. Block Diagram of Measurement Arrangement.

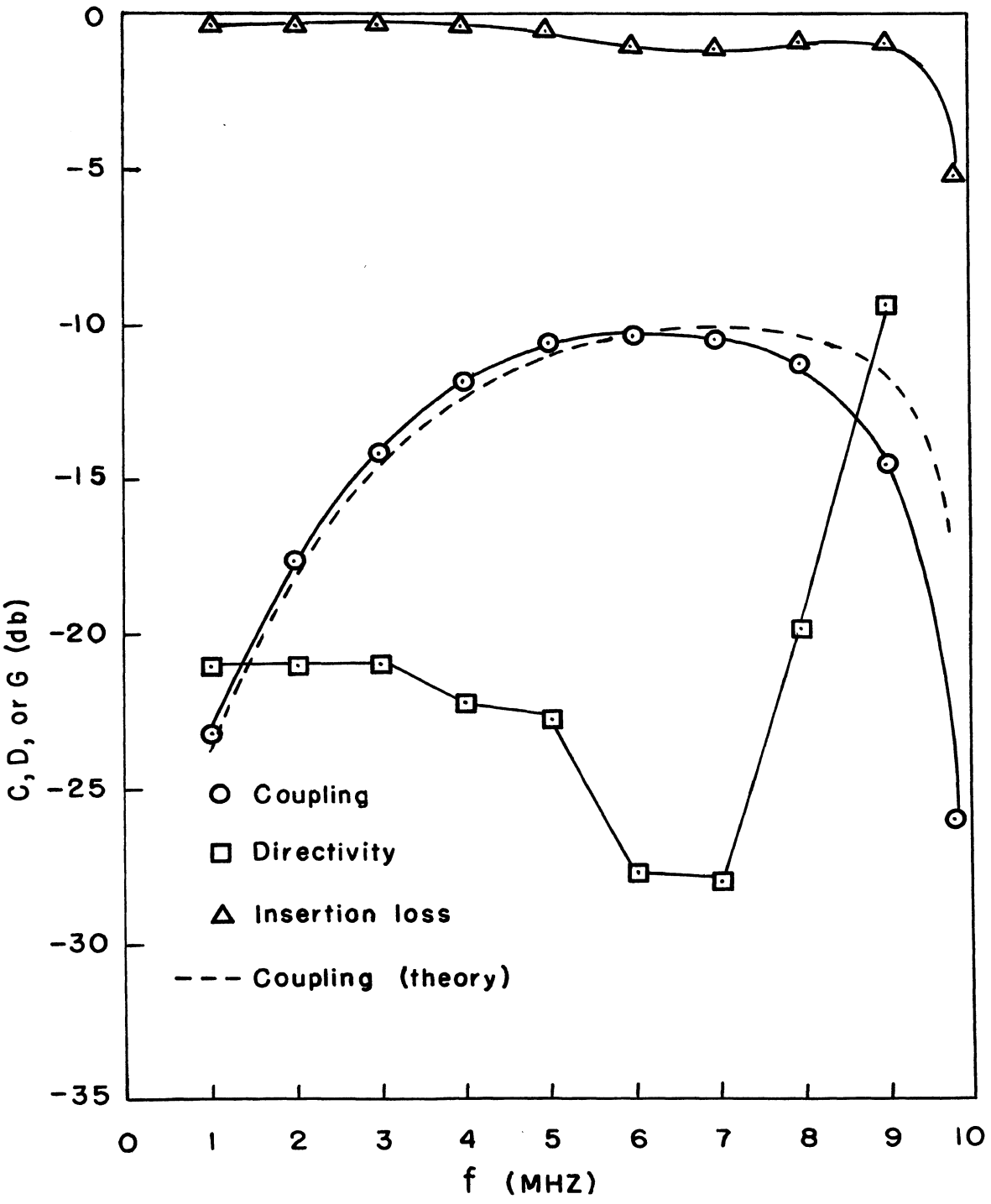

Figure 15. Measured Coupling, Directivity, and Insertion Loss Versus Frequency for a Single Section Coupler.

mismatch between the coupler and the matching network at the higher frequencies. This mismatch does not account for the poor directivity at the higher frequencies. The poor directivity is due mainly to the decrease in the coupled signal rather than to an increase in the signal at port four. The insertion loss is seen to be less than 1db except near the cutoff frequency where it increases rapidly. At this point the impedance of the coupler is approaching zero.

The coupling, directivity and insertion loss versus frequency for the two section coupler is shown in Figure 16. The dashed line in this figure is the coupling calculated from theory. The coupling is seen to follow closely the predicted value. Note that at the point where the coupling becomes small, the directivity has decreased. This is further evidence that the directivity is influenced more by the coupling than by the voltage at port four.

The insertion loss is less than 2db out to 8 MHz and then increases rapidly. Note that the insertion loss is larger for the two section coupler than for the single section coupler. This is due to the increase in resistance caused by the added section and becomes most noticeable as the characteristic impedance of the coupler decreases.

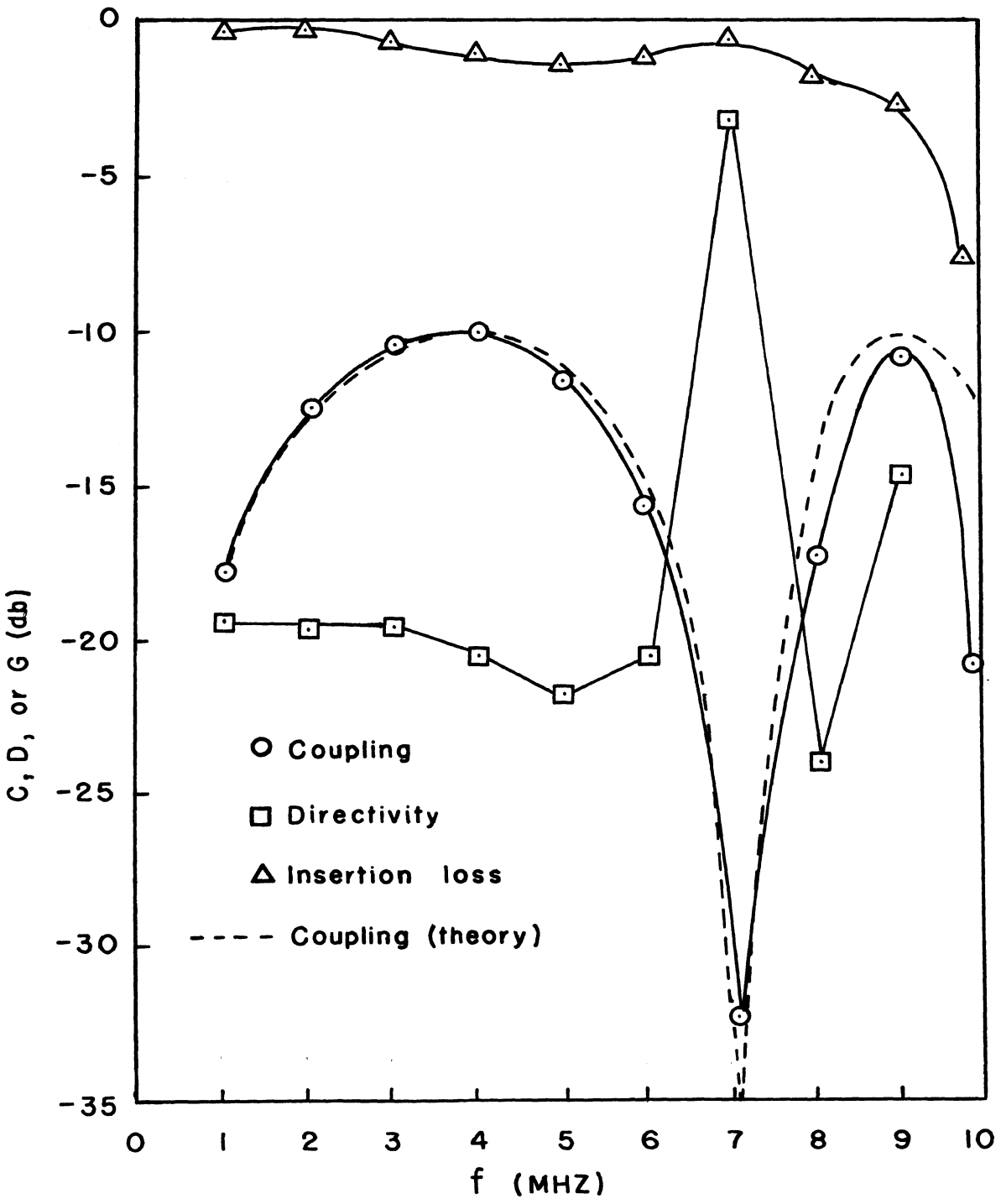

Figure 16. Measured Coupling, Directivity, and Insertion Loss Versus Frequency for a Two Section Coupler.

Figure 17 is a plot of the coupling, directivity, and insertion loss versus frequency for the three section coupler. The insertion loss is larger in this coupler than the other two couplers due to the added resistance of the third section. The coupling, in general follows the predicted value but note the decrease in the height of each successive peak. This is again an effect of the increased resistance and may to a certain extent be caused by the transformers not being purely inductive but with interwinding capacitance. The directivity in this case is seen to be poor.

The insertion loss can be decreased by using larger gauge wire in the coils of the matching network and in the transformers of the coupler. This may also increase the interwinding capacitance. The poor directivity and the notches in the coupling curves of the multisection couplers can be improved by using sections with different coupling coefficients.

In general, measured data follows that predicted by theory. Since the couplers are not ideal, a finite directivity is expected.

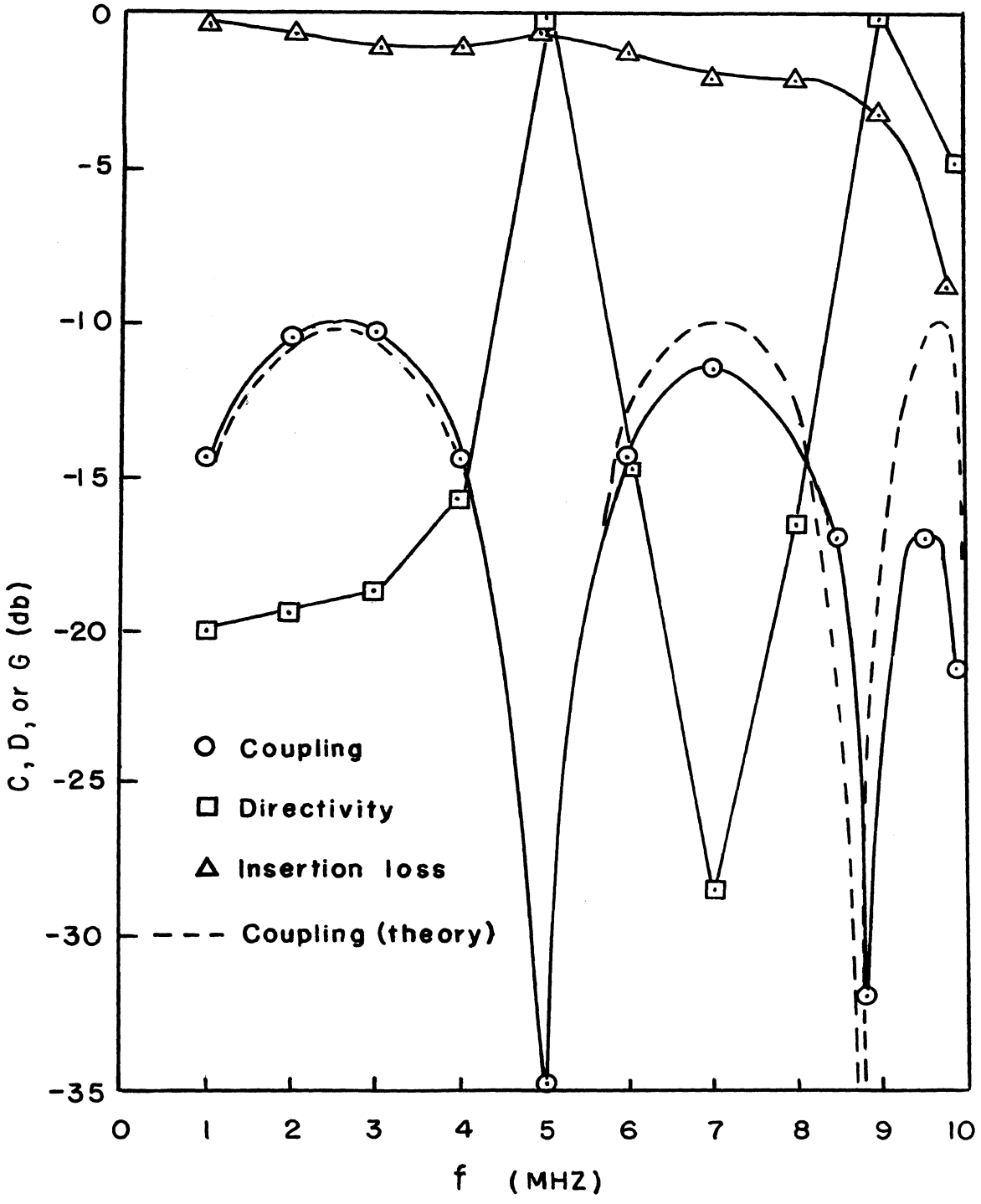

Figure 17. Measured Coupling, Directivity, and Insertion Loss Versus Frequency for a Three Section Coupler.

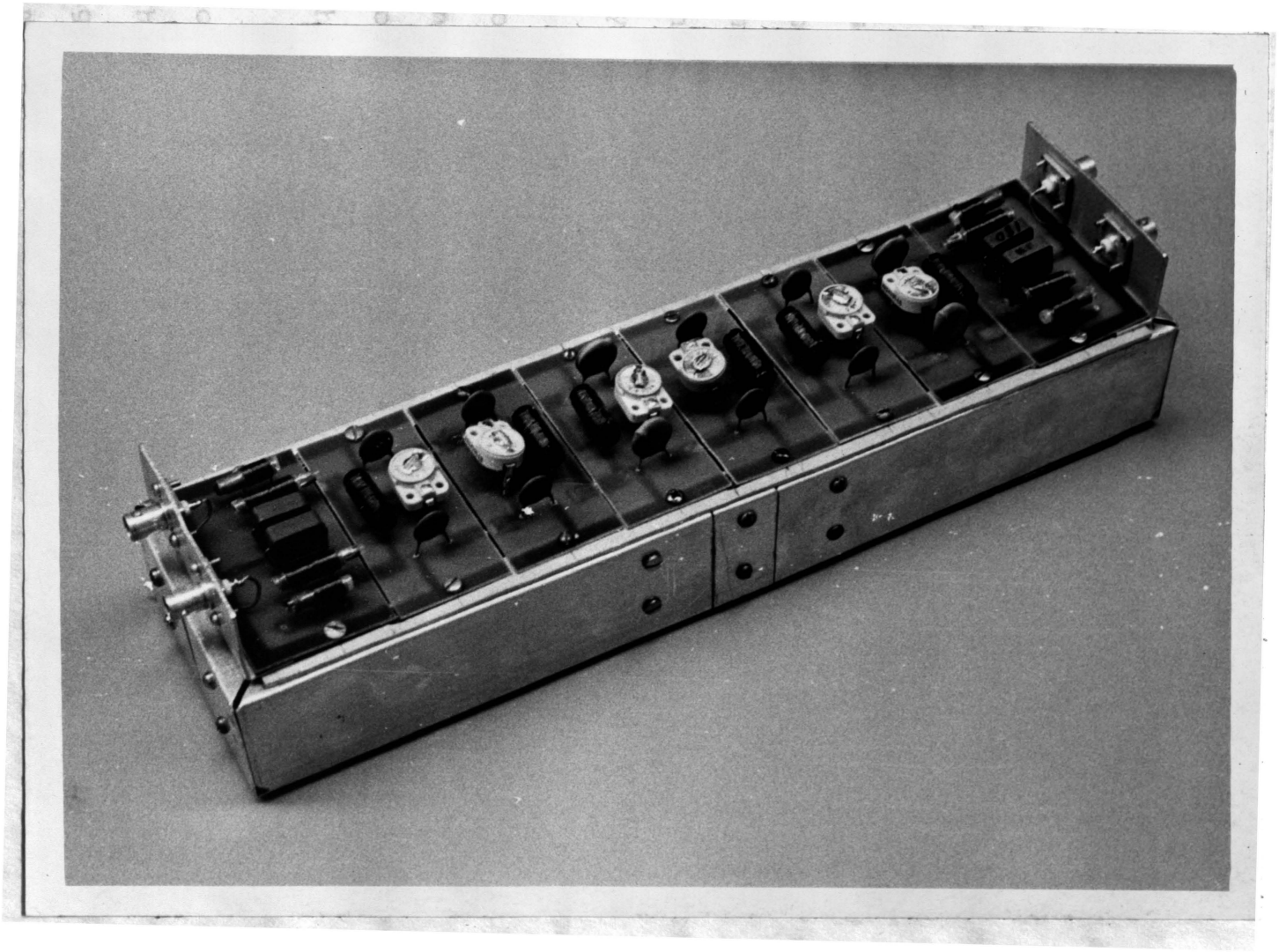

Figure 18. Prototype of the Three Section Directional Coupler With its Matching Network.

IV. SUMMARY AND CONCLUSIONS

A model of a lumped element directional coupler has been developed by considering a section of coupled transmission lines. A scattering matrix for one and two section couplers was obtained from the voltage-current equations by converting these equations to coupled-mode equations. Expressions for the coupling, directivity and insertion loss were obtained from the scattering matrix.

It was shown that the bandwidth was increased by using multiple sections but that a different coupling coefficient for one of the sections was needed to shape the coupling curve. The coupling, directivity, and insertion loss for three section couplers could be obtained by computer solution.

A method of determining the component values necessary to construct a coupler were presented. It was shown that an m-derived matching network was necessary to match the coupler to a constant impedance line. This network was then developed.

Data was presented for the one, two, and three section couplers for the case of identical sections. It was shown that, in general the measured data and the theory were in agreement. Differences in theory and experiment could be improved by reducing the resistance in the circuit.

Coupling at frequencies below the VHF range is possible by using a lumped element directional coupler. This

type of coupler eliminates the large physical size required by distributed parameter couplers at these frequencies. The lumped element couplers were shown to provide good bandwidth and high directivity.

V. SUGGESTIONS FOR FURTHER STUDY

The preceeding work has raised additional questions in the study of low frequency lumped element directional couplers. The following are some suggestions for additional study.

First, is it possible to interchange the L's and the C's to obtain a high pass type of coupler? This should provide a much wider bandwidth. The upper cutoff frequency should be limited only by stray and interwinding capacitance of the transformers.

Second, determine an analytic expression for the characteristic impedance of two and three section couplers for the case of non-identical coupling coefficients. This expression is needed to determine the proper network to match the coupler to a constant impedance line.

Third, obtain an analytic expression for the coupling of a three section coupler having different coupling coefficients for each section. This expression should be minimized with respect to the coupling coefficients to provide a wide bandwidth, minimum ripple coupler.

Fourth, determine a method for winding the transformers which will allow one to easily obtain the designed values.

BIBLIOGRAPHY

1. Mumford, W. W., "Directional Couplers", Proc. IRE, vol. 35, pp. 160-165; February, 1947.

2. Riblet, H. J., "A Matrix Theory of Directional Couplers", Proc. IRE, vol. 35, pp. 1307-1313; November, 1947.

3. Firestone, W. L., "Analyses of Transmission Line Directional Couplers", Proc. IRE, vol. 42, pp. 1529-1538; October, 1954.

4. Oliver, B. M., "Directional E. M. Couplers", Proc. IRE, vol. 42, pp. 1686-1692; November, 1954.

5. Shimizu, J. K. and Jones, E. M. T., "Coupled Transmission Line Directional Couplers", IRE Trans. on Microwave Theory and Techniques, vol. MTT-6, pp. 403-410, October, 1958.

6. Miller, S. E. and Mumford, W. W., "Multi-Element Directional Couplers", Proc. IRE, vol. 40, pp. 1071-1078; September, 1952.

7. Cristal, E. G. and Young, L., "Theory and Tables of Optimum Symmetrical TEM-Mode Coupled-Transmission-Line Directional Couplers", IEEE Trans. on Microwave Theory and Techniques, vol. MTT-13, pp. 544-558, September, 1965.

8. Louisell, W. H., "Analysis of the Single Tapered Mode Coupler", Bell Systems Tech. Journal, vol. 34, pp. 853-870; July, 1955.

9. Jones, E. M. T. and Bolljahn, J. T., "Coupled-Strip-Transmission Line Filters and Directional Couplers", IRE Trans. on Microwave Theory and Techniques, vol. MTT-4, pp. 75-81; April, 1956.

10. Gunderson, L. C. and Guida, A., "Stripline Coupler Design", Microwave Journal, vol. 8, pp. 97-101; June, 1965.

11. Toulios, P. P. and Todd, A. C., "Synthesis of Symmetrical TEM-Mode Directional Couplers", IEEE Trans. on Microwave Theory and Techniques, vol. MTT-13, pp. 536-544; September, 1965.

12. Miller, S. E., "Coupled Wave Theory and Waveguide Applications", Bell System Tech. Journal, vol. 33, pp. 677-692; May, 1954.

13. Cohn, S. B., "The Re-entrant Cross Section and Wide Band 3-db Hybrid Coupler", IEEE Trans. On Microwave Theory and Techniques, vol. MTT-11, pp. 254-258; July, 1963.

14. Pon, Chuck Y., "A Wide-Band 3-db Hybrid Using Semi-Circular Coupled Cross-Sections", Microwave Journal, vol. 12, 10; October, 1969.

15. Daly, D. A., Knight, S. P., Caulton, M., and Ekholdt, R., "Lumped Elements in Microwave Integrated Circuits", IEEE Trans. on Microwave Theory and Techniques, vol. MTT-15, pp. 713-721, December 1967.

16. Caulton, Martin, "The Lumped Element Approach to Microwave Integrated Circuits", Microwave Journal vol. 13, 5; May, 1970.

17. Murray-Lasso, M. A., "Unified Matrix Theory of Lumped and Distributed Directional Couplers", Bell Systems Tech. Journal, vol. 36, pp. 39-71; January, 1968.

18. Pierce, J. R., "Coupling of Modes of Propagation", Jour. Appl. Phys., vol. 25, pp. 179-183; February, 1954.

19. Adair, J. E. "Coupled-Mode Analysis of Nonuniform Coupled Transmission Lines", Technical Report 106, Electron Physics Laboratory, University of Michigan; March, 1968.

20. Van Valkenburg, M. E., Network Analysis. Englewood Cliffs: Prentice-Hall, Inc., 1959.

VITA

Constantine R. Jenkins was born on December 8, 1933, in New Orleans, Louisiana where he received his primary and secondary education. He received his college education from the University of Missouri-Rolla, Rolla, Missouri, where he received a Bachelor of Science Degree in Electrical Engineering in December, 1970. He has been enrolled in the Graduate School of the University of Missouri-Rolla since September, 1970.

Mr. Jenkins received an Associate in Science Degree in Electronic Engineering Technology from Central Technical Institute, Kansas City, Missouri in November, 1963. He has been employed in industry for many years.